

See discussions, stats, and author profiles for this publication at: <https://www.researchgate.net/publication/259764782>

Design, Synthesis, and Pharmacological Evaluation of a Novel Series of Pyridopyrazine-1,6-dione γ -Secretase Modulators

ARTICLE in JOURNAL OF MEDICINAL CHEMISTRY · JANUARY 2014

Impact Factor: 5.45 · DOI: 10.1021/jm401782h · Source: PubMed

CITATIONS

6

READS

56

21 AUTHORS, INCLUDING:



[Martin Pettersson](#)

Pfizer

23 PUBLICATIONS 298 CITATIONS

SEE PROFILE



[Douglas S Johnson](#)

Pfizer

59 PUBLICATIONS 2,201 CITATIONS

SEE PROFILE



[Kelly R Bales](#)

Pfizer

193 PUBLICATIONS 13,986 CITATIONS

SEE PROFILE



[Subas Sakya](#)

Bioduro (Shanghai) LLC

54 PUBLICATIONS 978 CITATIONS

SEE PROFILE

Design, Synthesis, and Pharmacological Evaluation of a Novel Series of Pyridopyrazine-1,6-dione γ -Secretase Modulators

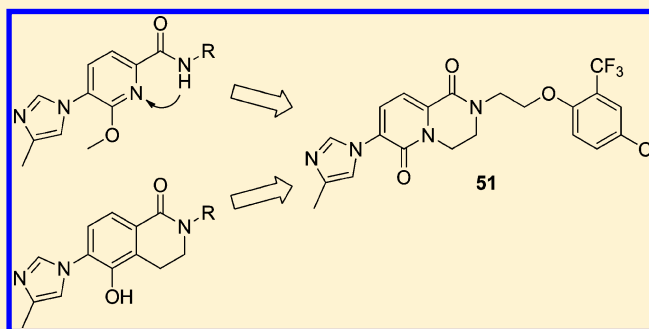
Martin Pettersson,^{*,†} Douglas S. Johnson,[†] Chakrapani Subramanyam,[‡] Kelly R. Bales,[†] Christopher W. am Ende,[‡] Benjamin A. Fish,^{‡,§} Michael E. Green,[†] Gregory W. Kauffman,[†] Patrick B. Mullins,[‡] Thayalan Navaratnam,^{‡,#} Subas M. Sakya,^{‡,||} Cory M. Stiff,[‡] Tuan P. Tran,[‡] Longfei Xie,[‡] Liming Zhang,^{‡,⊥} Leslie R. Pustilnik,[‡] Beth C. Vetelino,[‡] Kathleen M. Wood,[†] Nikolay Pozdnyakov,[†] Patrick R. Verhoest,[†] and Christopher J. O'Donnell[‡]

[†]Pfizer Worldwide Research & Development, 610 Main Street, Cambridge, Massachusetts 02139, United States

[‡]Pfizer Worldwide Research & Development, Eastern Point Road, Groton, Connecticut 06340, United States

S Supporting Information

ABSTRACT: Herein we describe the design and synthesis of a novel series of γ -secretase modulators (GSMs) that incorporates a pyridopyrazine-1,6-dione ring system. To align improved potency with favorable ADME and in vitro safety, we applied prospective physicochemical property-driven design coupled with parallel medicinal chemistry techniques to arrive at a novel series containing a conformationally restricted core. Lead compound **51** exhibited good in vitro potency and ADME, which translated into a favorable in vivo pharmacokinetic profile. Furthermore, robust reduction of brain A β 42 was observed in guinea pig at 30 mg/kg dosed orally. Through chemical biology efforts involving the design and synthesis of a clickable photoreactive probe, we demonstrated specific labeling of the presenilin N-terminal fragment (PS1-NTF) within the γ -secretase complex, thus gaining insight into the binding site of this series of GSMs.



■ INTRODUCTION

Alzheimer's disease (AD), first described in 1906 by German neuropathologist and psychiatrist Alois Alzheimer, is a progressive, neurodegenerative disorder that leads to cognitive impairment, loss of motor function, and ultimately death. Current therapies such as acetylcholinesterase inhibitors and NMDA receptor antagonists temporarily reduce the symptoms of AD but do not affect progression of the underlying disease. Currently, 1 in 8 people in America over the age of 65, or 5.2 million people, are affected by AD, and this number is expected to more than double by 2040 as the population ages.¹ AD represents a significant burden to the afflicted patients, caregivers, and the healthcare system, and effective treatments to reduce or halt the progression of this devastating disease present a major unmet medical need.

Genetic and histopathological evidence points to the aberrant production and accumulation of amyloid β (A β) peptides as a causative process in AD.² Oligomers of A β 42 have been shown to be neurotoxic in vitro, and these hydrophobic species have a high propensity for aggregation to generate insoluble amyloid plaques, a hallmark of AD pathology.³ Formation of A β 42 is initiated by cleavage of the amyloid precursor protein (APP) by the β -aspartyl secretase cleaving enzyme (BACE). The resultant membrane-bound C-terminal fragment undergoes a subsequent cleavage by γ -secretase to

afford amyloid peptides ranging from 37 to 43 amino acids in length. Thus, suppression of the de novo synthesis of neurotoxic A β 42 peptides via inhibition of BACE and/or modulation of γ -secretase represents a promising therapeutic avenue for the treatment of AD.⁴ Consequently, this approach is being aggressively pursued throughout the pharmaceutical industry as well as in academic laboratories.

Development of γ -secretase inhibitors (GSIs) has provided agents that successfully reduced A β in cerebrospinal fluid (CSF) in humans;⁵ however, a phase III study with GSI LY450139 (semagacestat) was recently halted due to adverse events including decline in cognition and increased incidence of skin cancer.⁶ Likewise, development of BMS-708,163 (avagacestat) was terminated after completion of phase II trials in which gastrointestinal and skin-related adverse events were observed.⁷ Part of the explanation for these failures may be that, in addition to APP, γ -secretase cleaves multiple other substrates; inhibition of such processing may result in detrimental side effects. For example, S3 cleavage of the Notch 1 receptor by γ -secretase within the membrane domain releases the notch intracellular domain (NICD). This translocates to the nucleus, where it activates transcription of target genes that play an

Received: November 17, 2013

Published: January 15, 2014

important role in cell differentiation including neuronal development.⁸ Inhibition of Notch processing by GSIs is thought to be responsible, at least in part, for the gastrointestinal adverse events and increased risk of skin cancer that have been observed in the clinic. Furthermore, the accumulation of APP β -C-terminal fragment (β -CTF) that results from γ -secretase inhibition has been implicated in neurotoxicity.⁹

In contrast to GSIs, γ -secretase modulators (GSMs) selectively alter the cleavage site of APP to reduce the formation of the neurotoxic peptides A β 42 and in many cases A β 40 as well, while increasing formation of A β 37 and/or A β 38, which are less prone to aggregation. Importantly, processing of other substrates including Notch 1 is not inhibited by GSMs.¹⁰ Furthermore, GSMs do not cause an accumulation of γ -secretase substrates such as the APP β -CTF. Focus has therefore shifted away from GSIs in favor of the development of GSMs, which may offer an improved safety profile.¹¹ Early efforts focused on lipophilic acid derivatives such as (R)-flurbiprofen (**1**, Figure 1), which originated from nonsteroidal

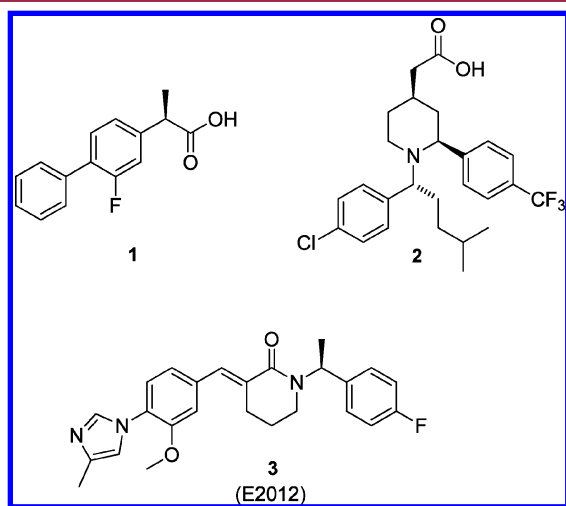


Figure 1. Representative acid GSMs **1**, **2**, and heteroaryl GSM **3**.

anti-inflammatory agents (NSAIDs).^{10b} Although **1** entered clinical development, it was unsuccessful in slowing cognitive decline in a phase III trial.¹² This may be attributed to its low in vitro potency (ca. 200 μ M) in combination with inadequate exposure at the target site due to poor brain penetration. Further efforts resulted in significant improvements in A β -lowering activity to afford acids such as **2** (GSM-1, A β 42 IC₅₀ value of 120–348 nM).¹³ However, examination of the patent literature suggests that a majority of the researchers in the field have shifted their efforts away from the NSAID-derived acids in favor of nonacid or heteroaryl-type series of GSMs, as exemplified by **3** (E2012).^{11a,b} This chemotype was initially discovered at Neurogenetics and was further developed by scientists at Eisai, who advanced **3** into phase I clinical trials.¹⁴ Further development of this compound was halted in favor of a second generation analogue with an improved potency and safety profile.

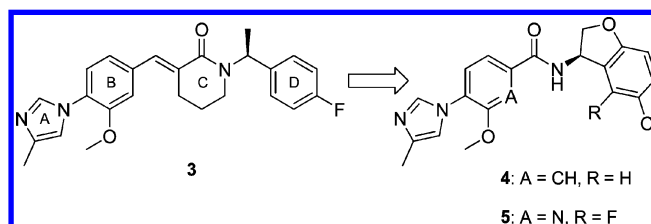
γ -Secretase is an intramembrane-cleaving aspartyl protease that is composed of four subunits: presenilin, Pen-2, Aph-1, and nicastrin.¹⁵ Although the exact mechanism of APP processing by γ -secretase is unknown, we and others have developed photoaffinity probes from both the acid and arylimidazole series of GSMs and demonstrated that these compounds bind to the

N-terminal fragment of presenilin (PS1-NTF) at distinct binding sites.^{13b,c,16} Importantly, GSIs did not compete with photolabeling of presenilin using either acid or imidazole probes, indicating that these GSMs do not share the binding site(s) of GSIs. As an aspartyl protease located within the membrane, γ -secretase presents a formidable challenge for the development of potent modulators with aligned absorption, distribution, metabolism, and excretion (ADME) attributes along with favorable physicochemical properties. This is evident when examining the patent literature, where on average, GSMs have significantly higher lipophilicities and molecular weights as compared to marketed CNS drugs.^{11a,b}

RESULTS AND DISCUSSION

We have previously described our efforts in the heteroaryl series using **3** as a starting point (Scheme 1).^{17,18} A β 42 IC₅₀ = 143

Scheme 1. Evolution of the Amide Series from Heteroaryl GSM **3**

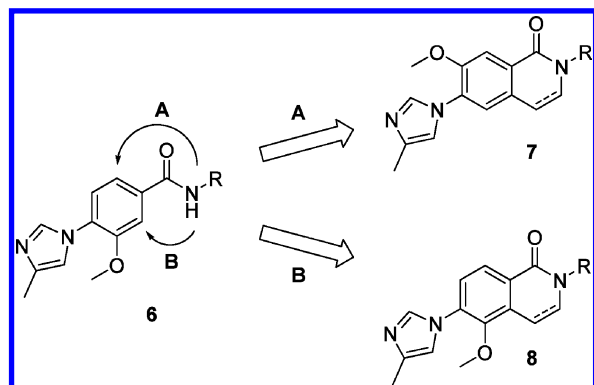


nM, clogP = 4.8,¹⁹ lipophilic efficiency (LipE) = 2.3,²⁰ and a central nervous system multiple parameter optimization score (CNS MPO) = 3.7/6.0.²¹ Our primary design objectives were to remove the cinnamide olefin and to improve overall physicochemical properties. In particular we sought to reduce lipophilicity, as a high clogP value has been linked to increased promiscuity and a higher risk of adverse findings in exploratory toxicology studies.²² Furthermore, targeting less lipophilic, more polar chemical space may increase the probability of achieving good alignment of potency with critical ADME parameters such as clearance, permeability, and brain penetration.^{21,23} These efforts resulted in the discovery of the dihydrobenzofuran amide series exemplified by **4** (A β 42 IC₅₀ = 521 nM, clogP = 3.96, LipE = 3.55, CNS MPO = 4.8) and **5** (A β 42 IC₅₀ = 188 nM, clogP = 3.96, LipE = 4.12, CNS MPO = 4.8).¹⁷ Both compounds demonstrated robust reduction of brain A β 42 at 100 mg/kg in guinea pig, and while **5** is less potent than **3**, it achieved an improvement in LipE of approximately two log units. However, our efforts to further improve potency through additional optimization of the right-hand dihydrobenzofuran amide moiety, while maintaining favorable alignment of ADME and physicochemical properties, were unsuccessful. Furthermore, the in vitro safety profile of this series emerged as a significant concern: although **4** and **5** did not pose a DDI risk, with IC₅₀ values for inhibition of CYP 2D6 and 3A4 greater than 30 μ M, CYP inhibition increasingly became a problem with more potent GSMs in this series. This finding is consistent with observations in related heteroaryl series reported in the literature.^{18a}

Given the challenges of aligning potency, clearance, brain penetration, and in vitro safety (DDI) in the amide series, we opted to focus our efforts on modifying the arylimidazole A-B moiety through design of a novel, conformationally restricted core with increased polarity. By introducing conformational constraint, we anticipated the opportunity to (a) lock the

molecule into the putative active conformation and therefore increase potency, and (b) reduce rotatable bonds and the number of hydrogen bond donors, which should improve permeability and brain penetration. As shown in Scheme 2,

Scheme 2. Design of Constrained Amide GSMs



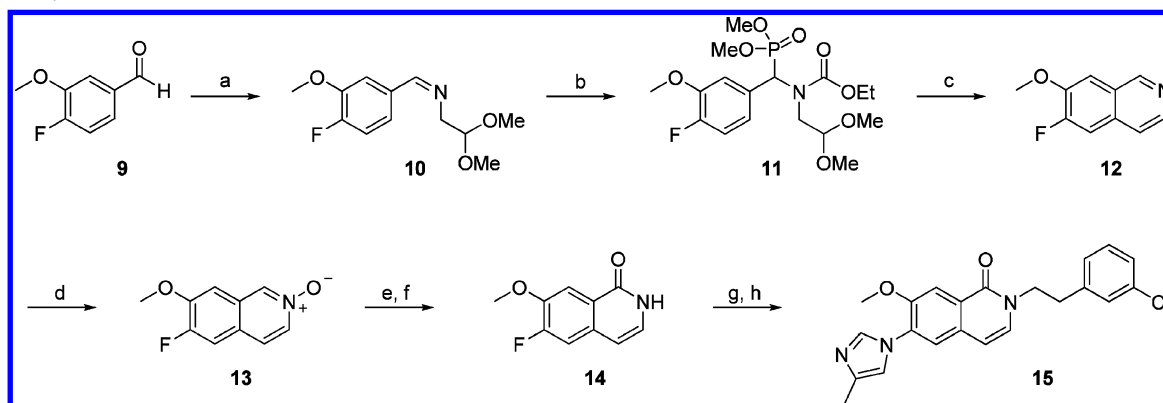
constraining the amide moiety of **6** by tying back the nitrogen onto the aryl ring forms a bicyclic core. Given the presence of the methoxy group, which is important for potency, this structural modification gives rise to two possible regioisomers, exemplified by **7** and **8**. Preparation of both of these novel cores would therefore provide valuable insights into the GSM pharmacophore, as it would lock the methoxy group and lactam carbonyl on either the same or opposite sides of the bicyclic ring system. The arylimidazole region of the non-NSAID derived GSMs is highly conserved, and only limited exploration of the aryl core had been exemplified in the GSM patent literature at the time.^{11a,b}

The synthesis of **15**, an example of regioisomer **7**, involved the rearrangement of an isoquinoline *N*-oxide as a key step (Scheme 3). Imine **10**, obtained from the condensation of aldehyde **9** with 2,2-dimethoxyethanamine, could not be directly cyclized to isoquinoline **12**. This transformation, known as the Pomeranz–Fritsch reaction,²⁴ typically works best with aromatic systems bearing multiple electron-donating substituents. One of the observed side reactions in this case involved hydrolysis of **10** back to aldehyde **9** under the acidic reaction conditions. This problem was circumvented by first

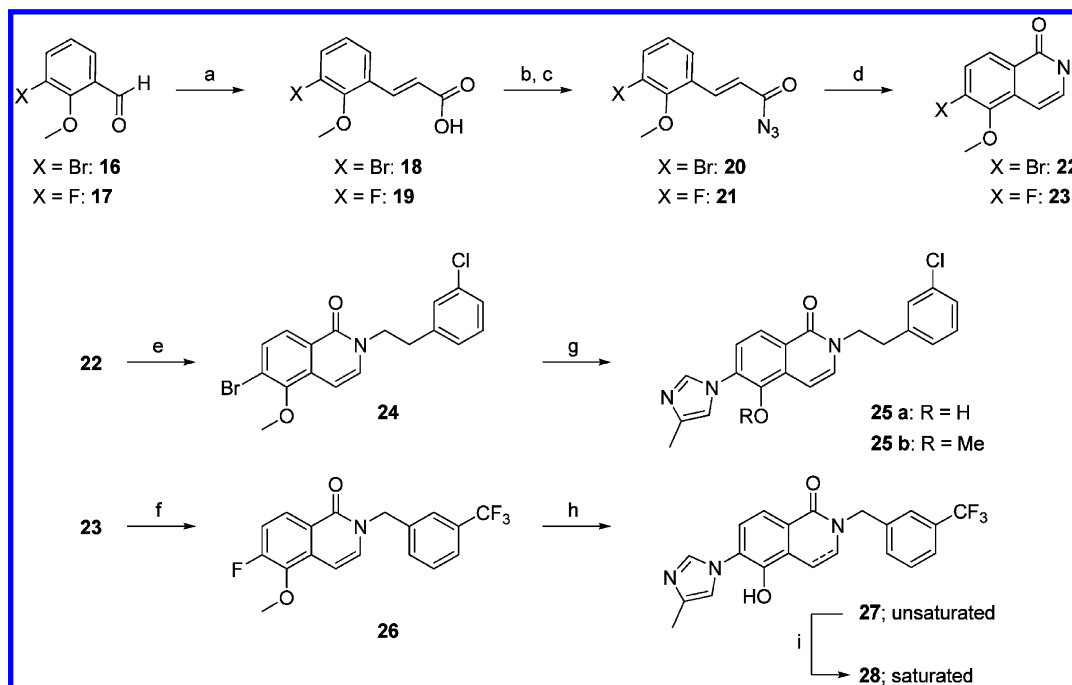
masking imine **10** as the carbamate phosphonate **11** prior to cyclization.²⁵ Thus, refluxing **11** in dichloromethane in the presence of TiCl_4 afforded isoquinoline **12** in good yield as a single regioisomer. Next, oxidation with *m*-CPBA furnished isoquinoline *N*-oxide **13**, which underwent a rearrangement to form isoquinolone **14** upon refluxing in acetic anhydride; this was followed by hydrolytic removal of the acetate group with sodium hydroxide. Following *N*-alkylation to introduce the side chain, the 4-methylimidazole moiety was installed via a nucleophilic aromatic substitution. This reaction was complicated by the presence of the methoxy substituent ortho to the aryl fluoride. Nevertheless, heating a mixture of fluoroquinolone, 4-methylimidazole, and potassium carbonate in DMSO to 135 °C afforded the target compound **15**, along with the corresponding regioisomeric imidazole adduct (not shown) in a 2.5:1 ratio, in 53% yield; this mixture was readily separable by preparative HPLC.

Synthesis of the 5,6-disubstituted isoquinolones **25a** and **25b**, examples of regioisomer **8**, commenced via condensation of aldehyde **16** with malonic acid, followed by decarboxylation to furnish **18** (Scheme 4). The carboxylic acid was then converted to the acyl azide **20** in preparation for the key tandem Curtius rearrangement/Friedel–Crafts acylation. In contrast to the transformation using diphenylphosphoryl azide (DPPA), the acyl azide was prepared in excellent overall yield by using thionyl chloride followed by addition of sodium azide. With acyl azide **20** in hand, the Curtius rearrangement/intramolecular Friedel–Crafts cascade afforded the 5,6-disubstituted isoquinolone intermediate **22** in 51% yield over three steps. The synthesis was then completed by alkylation with 1-(2-bromoethyl)-3-chlorobenzene followed by CuI-mediated coupling with 4-methylimidazole. Interestingly, the latter transformation resulted in complete demethylation of the methoxy group when the reaction mixture was heated at 130 °C: hydroxy-substituted quinolone **25a** was isolated in 74% yield as a 4:3 mixture of imidazole regioisomers, which were readily separated by preparative-HPLC. The demethylation could be suppressed by reducing the temperature to 100 °C, affording **25b** in 20% yield after separation of regioisomers by preparative-HPLC. The synthesis of 3-trifluoromethylbenzyl analogue **27** was completed in an analogous manner. Finally, the double bond of the isoquinolone in **27** was reduced via H-Cube flow hydrogenation to afford the saturated analogue **28**.

Scheme 3. Synthesis of **15^a**



^aReagents and conditions: (a) 2,2-dimethoxyethanamine, toluene, reflux; (b) EtOCOCl , THF, -10 °C to rt; then P(OMe)_3 ; (c) TiCl_4 , dichloromethane, reflux, 57% over three steps; (d) *m*-CPBA, dichloromethane, rt, 46%; (e) Ac_2O , reflux; (f) sodium hydroxide, 100 °C, 84% over two steps; (g) NaH, 1-(2-bromoethyl)-3-chlorobenzene, DMA, rt, 62%; (h) 4-methylimidazole, K_2CO_3 , DMSO, 135 °C, 7%.

Scheme 4. Synthesis of 25b, 27, and 28^a

^aReagents and conditions: (a) malonic acid, piperidine, pyridine, 120 °C, 50% (**18**), 19% (**19**); (b) SOCl₂, rt, then 90 °C; (c) NaN₃, H₂O, acetone, 0 °C; (d) 1,2-dichlorobenzene, 140 °C, 1 h; then catalytic I₂, 185 °C, 1.5 h, 51% (**22**, three steps), 16% (**23**, three steps); (e) NaH, 1-(2-bromoethyl)-3-chlorobenzene, DMA, rt 45%; (f) NaH, 3-CF₃-benzyl bromide, DMA, rt, 97%; (g) 4-methylimidazole, CuI, Cs₂CO₃, DMF, 100 °C, 20%; (h) 4-methylimidazole, K₂CO₃, DMF, 120 °C, 27%. (i) H₂, Pd/C, H-Cube, 97%.

Next, we determined A β 42-lowering activity in a whole-cell assay using Chinese hamster ovary (CHO) cells that over-express wild type human APP (hereafter expressed as A β 42 IC₅₀). Key compounds were spot-checked for inhibition of Notch signaling in HEK 293 NdeltaE cells.²⁶ A majority of the analogues were also tested in several in vitro ADME assays, including stability in human liver microsomes.²⁷ The potential for P-glycoprotein (P-gp)-mediated efflux was examined by measuring the efflux ratio (MDR Er) in a Madin–Darby canine kidney (MDCK) cell line that had been transfected with the human MDR1 gene encoding P-gp.²⁸ Interestingly, constraining the amide according to path A (Scheme 2) to form **15** (Table 1) resulted in complete loss of activity, whereas cyclization according to path B to afford the isomeric lactam **25b** preserved A β 42-lowering activity (A β 42 IC₅₀ = 3.4 μ M). This finding provided valuable insight into the GSM pharmacophore, as it suggested that the two polar functional groups need to be situated on opposing sides of the scaffold to enable the key interactions with the binding site.

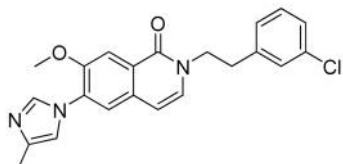
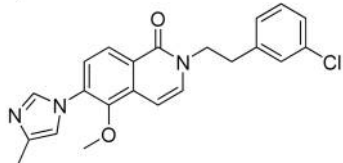
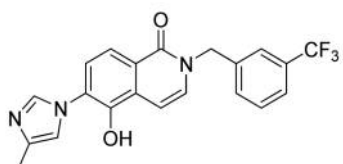
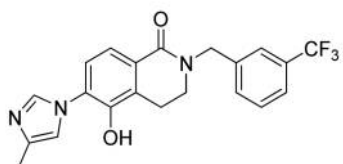
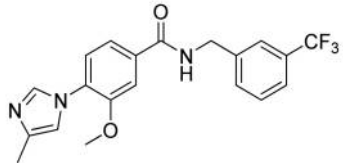
Next, we introduced a *m*-CF₃-benzyl substituent on the amide nitrogen, as we had observed in our amide series that *N*-benzyl groups generally have comparable potency to *N*-phenethyl groups but offer improved metabolic stability.¹⁷ During the S_NAr reaction to introduce the 4-methylimidazole moiety, the corresponding desmethyl (phenol) derivative **27** was isolated as the major product. Phenol **27** was found to be 3-fold more potent (A β 42 IC₅₀ = 920 nM) than **25b**. We previously observed in the amide series (e.g., **4** and **5**) that introduction of hydrogen bond donors, such as hydroxyl groups, generally results in increased P-gp liability as measured by an increased MDR Er liability when introduced onto the aryl core (B-ring) as opposed to the lipophilic right-

hand section of the molecule (C- and D-rings).¹⁷ Given these prior observations, we were intrigued to note that phenol **27** maintained a low MDR efflux ratio (MDR Er = 1.1). This provided the potential to incorporate polarity into the molecule and to bring the series into better physicochemical property space without impairing penetration into the brain.

We next sought to reduce the planarity of the bicyclic core by introducing sp³ centers into the system. Toward this end, **27** was subjected to hydrogenation, affording the saturated lactam **28**. This compound represented an important advancement for the program, as it successfully aligned moderate in vitro potency with an improved ADME profile: the A β 42 IC₅₀ of **28** compared favorably to that of the monocyclic parent amide **29**¹⁷ (0.40 μ M vs 0.66 μ M, respectively), while also maintaining a low MDR efflux ratio (MDR Er = 1.9) and good passive permeability (RRCK $P_{app,A \rightarrow B}$ = 10.4 $\times 10^{-6}$ cm/s).²⁹ Furthermore, **28** achieved excellent stability in human liver microsomes (HLM CL_{int,app} < 8.0 mL/min/kg). The presence of a phenol, however, was cause for some concern, as phenols are known to undergo secondary metabolism through glucuronidation.³⁰ Consequently, **28** was evaluated for metabolic stability in human hepatocytes and was found to have only moderate stability (HHEP CL_{int,app} = 90.5 mL/min/kg; $T_{1/2}$ = 19.3 min). This indirectly suggested that the phenol may indeed be a metabolic liability. Therefore, the next phase of the design process focused on identifying alternative heterocyclic templates that would maintain or increase the polarity while avoiding the liability associated with the phenol.

Evaluation of the heterocyclic cores that had been prepared thus far suggested that the bicyclic lactam of **28** (as its generalized template **31**) could be combined with the pyridyl amide core of **5** (as its generalized template **30**) (Scheme 5). Introduction of a two-carbon linker to connect the amide

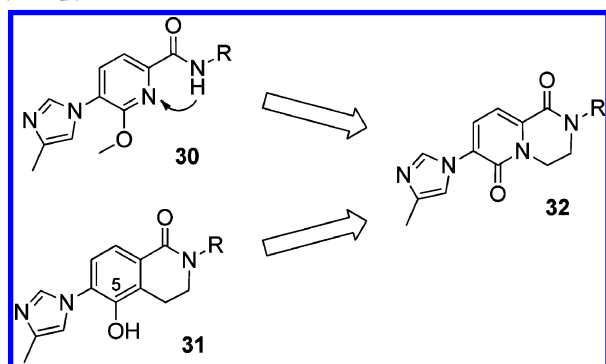
Table 1. In Vitro Pharmacology and Disposition Data for Constrained Amide GSMs

Compound	IC ₅₀ (Aβ42, μM) ^a	MDR Er ^b	HLM CL _{int,app} (mL/min/kg) ^c
15 	>15.8	1.0	32.7
25b 	3.4	1.2	36.1
27 	0.92	1.1	12.3
28 	0.40	1.9	<8.0
29 	0.66	1.8	27.8

^aAβ42 IC₅₀ values were obtained in a whole cell assay using CHO APP_{wt} cells. Aβ42 IC₅₀ values shown here are the geometric mean of at least three experiments. ^bMDR efflux ratio in a MDCK assay utilizing MDCK cells transfected with the gene that encodes human P-glycoprotein.²⁸

^cHuman liver microsome-derived intrinsic clearance.²⁷

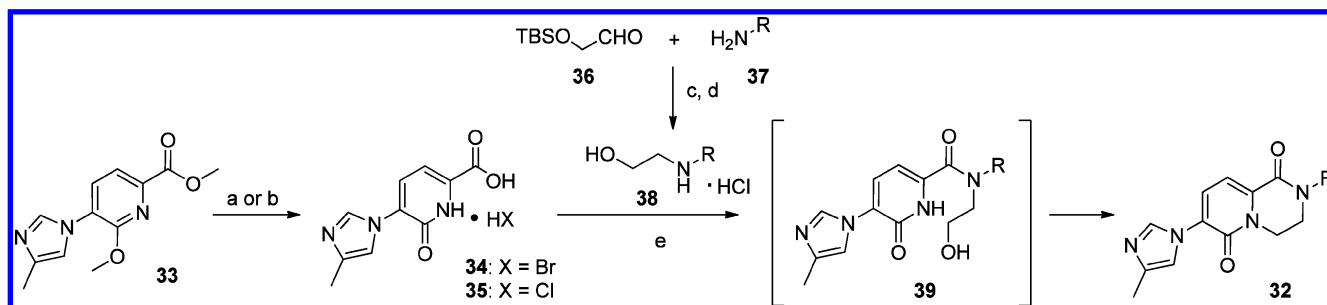
Scheme 5. Design Strategy Leading to a Novel Pyridopyrazine-1,6-dione Series



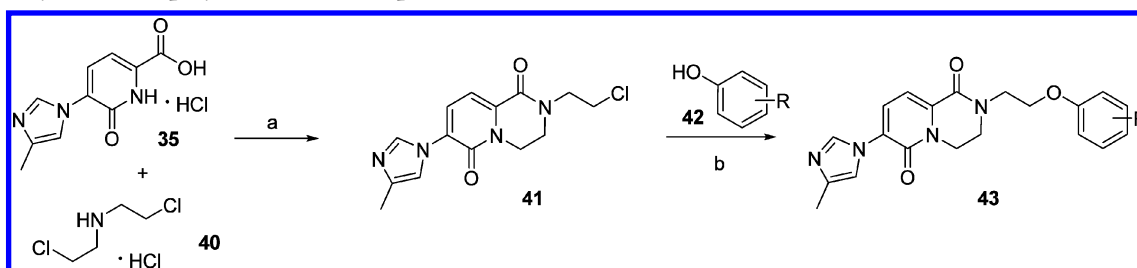
nitrogen of **30** to the pyridyl nitrogen would require conversion of the methoxypyridine into a pyridone, as shown in **32**. The resultant pyridopyrazine-1,6-dione structural motif maintains a polar functional group in the 5-position, allowing for increased potency and improved properties, but the carbonyl of the pyridone should not carry the metabolic liabilities associated

with a phenol. We therefore decided to invest in the development of an efficient synthetic route to this novel GSM core.

There are only a limited number of published synthetic approaches to bicyclic heterocycles related to pyridone **32**, none of which were directly applicable to incorporation of the requisite substitution pattern.³¹ We therefore developed a facile synthesis that features a novel one-pot, HATU³²-mediated amide coupling/cyclization reaction. Details of the development, scope, and limitations of this transformation have recently been described.³³ The known pyridyl ester **33**^{17,34} was heated in the presence of HBr and AcOH to afford the desired acid **34** as the HBr salt (Scheme 6). Alternatively, ester **33** could be converted to the HCl salt **35** in quantitative yield by heating in HCl/1,4-dioxane. Continuing from pyridone acids **34** or **35**, we had originally envisioned a stepwise approach whereby an amide coupling reaction would be carried out with amino alcohol **38** followed by conversion of the hydroxyl group to a suitable leaving group and finally intramolecular alkylation. To our surprise, subjecting a mixture of **34** or **35** and amino alcohol **38** (derived from 1-

Scheme 6. Synthesis Employed for Preparation of 44 and 45^a

^aReagents and conditions: (a) HBr, HOAc, 150 °C, 79%; (b) HCl, 1,4-dioxane, 150 °C, quant; (c) NaBH(OAc)₃, DIPEA, THF; (d) HCl, MeOH; (e) HATU, DIPEA, dichloromethane, rt, 30–80%.

Scheme 7. Synthesis Employed for Initial Preparation of 46–53^a

^aReagents and conditions: (a) HATU, K₂CO₃, DMF, 100 °C, 56%; (b) K₂CO₃, DMSO, 100 °C, 30–60%.

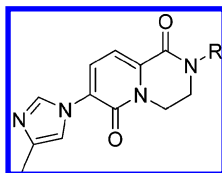
phenylethylamine) to 1 equiv of HATU in the presence of *N,N*-diisopropylethylamine (DIPEA) did not produce the targeted alcohol intermediate 39 as the major product (Scheme 6); instead, cyclized product 32 was isolated, as a mixture with 39 and unreacted acid 34 (3:2:5 ratio, respectively).³³ The cyclization step was found to be promoted by the HATU coupling reagent, and the one-pot conversion to 32 could be enhanced by running the reaction in the presence of 2.5 equiv of HATU. Further optimization resulted in a useful protocol that allowed access to a diverse set of pyridopyrazine-1,6-dione derivatives.³³ The utility of this transformation was further expanded by successfully incorporating parallel medicinal chemistry techniques and utilizing in situ monomer synthesis. We initially prepared the requisite amino alcohols 38 via reductive amination of ethanolamine with substituted benzaldehydes; however, the range of monomers that could be prepared using this approach was rather limited. Therefore, an improved sequence was developed that took advantage of the large diversity of our amine reagent collection. As shown in Scheme 6, reductive amination of various amines 37 with 2-(*tert*-butyldimethylsilyloxy)acetaldehyde (36) gave TBS-protected ethanolamine derivatives in good yield. These intermediates were then deprotected by exposure to methanolic HCl. The resulting HCl salts were obtained cleanly and could be used without further purification in the ensuing coupling reaction. An alternative to this approach involved monoalkylation of amines 37 with 2-bromoethanol. All three in situ monomer syntheses have been successfully applied to the preparation of pyridopyrazine-1,6-diones in parallel medicinal chemistry format.

We soon identified the phenoxyethyl moiety as an amide substituent warranting further investigation (*vide infra*) and elected to deconstruct this *enabled monomer* to facilitate SAR exploration of the aryl substitution pattern. Toward this end, we found that pyridone acid 35 underwent a one-pot coupling/

cyclization reaction with bis(2-chloroethyl)amine (40) to deliver chloroethyl derivative 41 in 42% yield (Scheme 7). With ready access to this valuable intermediate, we then carried out alkylations with a diverse set of phenols in parallel format. In particular, by running the alkylation reactions in DMSO as solvent, only a filtration was necessary upon completion of the reaction, whereupon the mixture could be directly purified via prep-HPLC; this protocol was ideal for rapid exploration of SAR on small scale. For the purpose of scale-up of key compounds, the preferred method involved the original coupling/cyclization reaction (*vide supra*) using amino alcohols prepared by alkylation of phenols with dibromoethane, followed by reaction with ethanolamine to provide the requisite compounds 38 (see Experimental Section).

With a facile approach to the novel pyridopyrazine dione GSM template in hand, we set out to explore SAR in this series. Compound 44, bearing a 3-CF₃-benzyl *N*-substituent, was prepared first, as a direct comparison to phenol 28. Although 44 was less potent than 28 (*A*_{β42} IC₅₀ = 1.6 μM vs 400 nM), it resided in superior physicochemical space as indicated by a CNS MPO of 5.7/6.0, versus 4.6/6.0 for phenol 28, and improvement in LipE from 2.3 to 3.5. Furthermore, 44 maintained excellent stability in human liver microsomes. Most importantly, the increase in polarity of 44 did not lead to an increase in P-gp efflux liability (MDR Er = 1.5). The favorable ADME and physicochemical property profile of 44, coupled with the fact that we had developed a facile, parallel-enabled synthesis, prompted further investigation of this series to determine the extent to which potency could be optimized. Consequently, GSM 45, which incorporated an extended linker, was rapidly identified. This compound demonstrated that reasonable potency (*A*_{β42} IC₅₀ = 410 nM) could indeed be attained within this series while maintaining excellent physicochemical properties (clogP = 2.52; CNS MPO = 5.6/6.0) and microsomal stability in HLMs (HLM CL_{int,app} = 8.1

Table 2. In Vitro Pharmacology and Disposition Data for Pyridopyrazine-1,6-dione GSMs



	R	IC ₅₀ (Aβ ₄₂ , nM) ^a	clogP	MDR Er ^b	HLM CL _{int,app} (mL/min/kg) ^c	RLM CL _{int,app} (mL/min/kg) ^d
44		1635	2.25	1.5	<8.0	<25.4
45		410	2.52	1.7	8.1	482
46		311	2.56	1.5	12.7	97.0
47		1498	2.05	1.5	<10.4	117
48		530	2.56	1.2	<8.0	79.4
49		1270	2.56	1.5	<9.7	40.3
50		252	2.75	1.5	<8.8	44.1
51		101	3.32	1.8	<8.0	47.6
52		15	2.85	1.5	30.0	469

^aAβ₄₂ IC₅₀ values were obtained in a whole cell assay using CHO APP_{wt} cells. Aβ₄₂ IC₅₀ values are the geometric mean of at least three experiments. ^bMDR efflux ratio using a MDR1/MDCK assay utilizing MDCK cells transfected with the gene that encodes human P-glycoprotein.²⁸

^cHuman liver microsome-derived intrinsic clearance.²⁷ ^dRat liver microsome-derived intrinsic clearance.

mL/min/kg). Furthermore, in contrast to phenol **28**, GSM **45** was also found to have very good stability in human hepatocytes (HHEP CL_{int,app} < 2.8 mL/min/kg), thus achieving one of the key design objectives that had prompted the development of this novel, conformationally constrained core.

A disadvantage to the extended linker of **45** was that it exhibited high turnover in rat liver microsomes (RLM CL_{int,app}

= 482 mL/min/kg) despite excellent human microsomal stability (HLM CL_{int,app} = 8.1 mL/min/kg). This was undesirable because many of our in vivo efficacy and safety studies are conducted in rodents. On the other hand, compound **46**, which incorporates a phenoxyethyl moiety as the amide N-substituent, was found to have improved rat microsomal stability (RLM CL_{int,app} = 97.0 mL/min/kg) along

with slightly improved potency ($A\beta_{42}$ IC_{50} = 311 nM). The presence of the phenol ether linkage in **46** rendered this substituent an *enabled monomer*, providing a valuable synthetic disconnection to facilitate further SAR efforts. This allowed us to use our extensive phenol monomer set to rapidly explore various substitution patterns using phenol alkylation chemistry in parallel (vide supra). As a result, we quickly established that an *o*-CF₃ group was key to optimal potency. For example, the corresponding *o*-chloro-substituted analogue **47** was >4-fold less active. Likewise, moving the CF₃ group to the meta- (**48**) or para-position (**49**) resulted in a loss of $A\beta$ -lowering activity. Compound **46** had the best overall in vitro profile thus far; however, it only exhibited 23% oral bioavailability in rat. We reasoned that this may in part be due to inadequate rat microsomal stability, leading to extensive first-pass metabolism. Furthermore, it was conceivable that the terminal aryl ring might undergo cytochrome P450 (CYP)-mediated hydroxylation in the para-position, as a result of activation by the electron-donating alkoxy linker. To test this hypothesis, GSM **50** was prepared, in which the metabolically labile para-position was blocked by a fluoro substituent. Not only was this compound more potent ($A\beta_{42}$ IC_{50} = 252 nM), but the rat microsomal clearance was reduced from 97.0 to 44.1 mL/min/kg. Moreover, this modification may have contributed to a significant improvement in rat oral bioavailability: compound **50** had 100% oral bioavailability, which stands in sharp contrast to the 23% found for desfluoro analogue **46**. In addition to low clearance (HLM $CL_{int,app}$ = 8.8 mL/min/kg), GSM **50** was found to have excellent permeability (RRCK $P_{app,A\rightarrow B}$ = 17.7×10^{-6} cm/s and $MDR_{A\rightarrow B}$ = 13.1×10^{-6} cm/s) as well as a low efflux ratio (MDR_{Er} = 1.5). In terms of physicochemical properties, **50** is considerably less lipophilic than **3** (cLogP = 2.75 vs 4.8), which contributes to an improvement CNS MPO and LipE relative to **3**. GSMs **50** and **3** have CNS MPO scores of 4.6 and 3.7, and LipE values of 3.6 and 2.3, respectively.

The design of the pyridopyrazine-1,6-dione series and the subsequent discovery of GSM **50** allowed us to significantly improve upon our previous amide series by successfully aligning potency, clearance, permeability, and MDR efflux ratio within excellent CNS property space. However, further gains in potency were necessary to approach an acceptable human dose projection. Toward this end we identified **51**, wherein the *p*-fluoro substituent of **50** has been replaced with a chloro substituent. GSM **51** maintained an in vitro ADME profile similar to that of **50**, but was more potent ($A\beta_{42}$ IC_{50} = 101 nM). This compared favorably to the reference compound **3** ($A\beta_{42}$ IC_{50} = 143 nM), which had served as the original starting point for our program. Compound **51** maintained good permeability (RRCK $P_{app,A\rightarrow B}$ = 10.5×10^{-6} cm/s and $MDR_{A\rightarrow B}$ = 5.8×10^{-6} cm/s) and low efflux ratio (MDR_{Er} = 1.8). Although **51** was more lipophilic (cLogP = 3.32) than **50**, it remained within good CNS physicochemical property space, as indicated by a CNS MPO score of 4.6. Additional chemistry efforts suggested that potency could be improved further in this series. For example, naphthyl analogue **52** had an $A\beta_{42}$ IC_{50} of 15 nM; however, this compound had insufficient stability in rat liver microsomal stability to warrant further studies. Ultimately, GSMs **50** and **51** were selected for further profiling in vitro and in vivo.

Table 3 summarizes the overall physicochemical profiles of **50** and **51**, which compare favorably to those of the majority of GSMs in the patent literature.^{11a} These compounds achieved adequate aqueous kinetic solubility, which in part may be

Table 3. Physicochemical Properties of GSMs **50** and **51**

	ClogP	log D ^a	TPSA	MW	CNS MPO ^b	solubility, pH 6.5 (μ M) ^c
50	2.75	2.98	69	450	5.35	177
51	3.32	3.12	69	466	4.64	95.6

^aShake flask log D.³⁵ ^bCentral nervous system multiple parameter optimization score.²¹ ^cKinetic solubility was measured at Analiza, Inc.³⁶

attributed to increased sp³/sp² ratio. An additional advantage of this series was an improvement in the cytochrome P450 inhibition profile, which had plagued the earlier phenylimidazole series;^{18a} GSMs **50** and **51** had IC_{50} values greater than 30 μ M against the major CYP isoforms, although they exhibited moderate inhibition of CYP 2C8 and CYP 2C9 (Table 4). Finally, in accordance with the typical profile of γ -secretase modulators, both lead compounds **50** and **51** were inactive against Notch (IC_{50} > 50 μ M). This was the case for all compounds in this series that were spot-checked for inhibition of Notch signaling.

The lead compounds exhibited good pharmacokinetic parameters in rat, including high oral bioavailability (%F), low to moderate clearance (CL), and reasonable half-life ($T_{1/2}$) (Table 5). When dosed orally at 5 mg/kg, **50** and **51** reached plasma concentrations of 964 ng/mL and 4140 ng/mL, respectively, at the 1 h time point. The lead compounds also exhibited acceptable brain penetration, as evidenced by unbound brain ($C_{b,u}$) to unbound plasma ($C_{p,u}$) concentration ratios of 0.43 and 0.32 for **50** and **51**, respectively. The extent to which GSM **51** was able to reduce $A\beta_{40/42}$ in vivo was evaluated in a guinea pig efficacy model. The compound was administered orally in doses of 10, 30, and 90 mg/kg, and levels of brain $A\beta_{42}$, $A\beta_{40}$, $A\beta$ total, and $A\beta_{38}$ were measured 4 h postdose along with compound exposure. As shown in Figure 2, de novo synthesis of brain $A\beta_{42}$ was reduced in a dose-dependent manner with reductions of 19%, 44%, and 68% at the 10, 30, and 90 mg/kg doses, respectively. Dose-dependent suppression of $A\beta_{40}$ was also observed, but the effect of **51** on $A\beta_{40}$ was slightly less than for $A\beta_{42}$. While there was a trend toward reduction of $A\beta$ total at the higher doses, this change was not statistically significant. Furthermore, at the highest dose, an increase in the formation of $A\beta_{38}$ was observed, which is consistent with the profile of a γ -secretase modulator. The $A\beta$ profile of a related compound in guinea pig brain was also examined by immunoprecipitation followed by MALDI-TOF MS (IP/MS) analysis of $A\beta$ peptides. $A\beta_{37}$ was found to be increased more than $A\beta_{38}$ (data not shown), which is consistent with what has been reported for other arylimidazole GSMs.^{14b,37}

To determine the target of this novel class of GSMs within the γ -secretase complex, we synthesized a clickable photoaffinity probe containing a benzophenone photoreactive group to effect covalent capture of the binding partner(s) upon UV irradiation and an alkyne handle to enable subsequent click chemistry-mediated conjugation of biotin (see Supporting Information).^{16,38} The resulting photoprobe, GSM-827-BPpyne (**53**), maintained good potency, exhibiting an $A\beta_{42}$ IC_{50} of 135 nM (Figure 3). With a promising photoprobe in hand, we performed photoaffinity labeling studies in HeLa cell membranes, which are known to have high γ -secretase activity.^{13c,16b,c} The photoprobe **53** was incubated with HeLa cell membranes in the presence or absence of GSM or GSI

Table 4. CYP Inhibition by GSMs 50 and 51

	CYP 1A2 IC ₅₀ (μM)	CYP 2C19 IC ₅₀ (μM)	CYP 2C8 IC ₅₀ (μM)	CYP 2C9 IC ₅₀ (μM)	CYP 2D6 IC ₅₀ (μM)	CYP 3A4 IC ₅₀ (μM)
50	>30.0	>30.0	19.0	>30.0	>30.0	>30.0
51	>30.0	>30.0	12.3	15.4	>30.0	>30.0

Table 5. Pharmacokinetic Profile of GSMs 50 and 51 in Rat

	CL (mL/min/kg) ^a	T _{1/2} (h) ^a	Vdss (L/kg) ^a	%F ^b	plasma concentration (ng/mL) ^c	brain concentration (ng/mL) ^c	B/P ^c	C _{b,u} /C _{p,u} ^d
50	14.3	2.09	1.91	100	964	718	0.74	0.43
51	1.41	6.88	0.69	88	4140	1000	0.24	0.32

^aDetermined from 1 mg/kg intravenous dose. ^bCalculated using the exposure from 1 mg/kg intravenous dose and 5 mg/kg oral dose. ^c5 mg/kg oral dose, 1 h time point. ^dPlasma free fractions in rat for 50 and 51 were 5.5% and 0.63%, respectively, and rat brain free fractions for 50 and 51 were 3.2% and 0.84%, respectively.

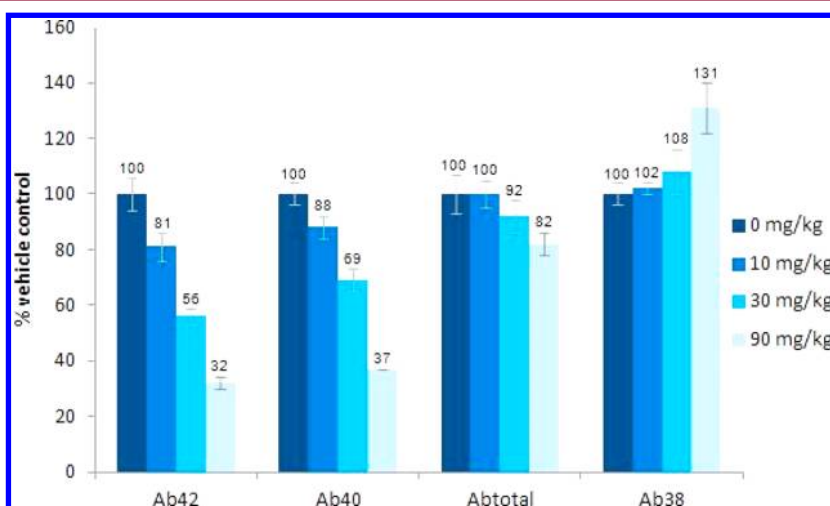


Figure 2. Dose–response of 51 in guinea pig efficacy model reported as percent of vehicle.

Table 6. Plasma, Brain, and CSF Exposure of GSM 51 in the Guinea Pig Efficacy Model, at 4 h Postdose

dose (po, mg/kg)	plasma (μM) ^a	brain (μM) ^b	CSF (nM)
10	0.367 ± 0.182	2.91 ± 1.39	12.7 ± 7.2
30	0.819 ± 0.056	9.16 ± 4.91	35.7 ± 5.9
90	7.30 ± 2.76	52.4 ± 17.6	239 ± 57

^aFree fraction of 51 in guinea pig plasma ($F_{u,p}$) was 7%. ^bFree fraction of 51 in guinea pig brain ($F_{u,b}$) was 0.8%.

competitor compounds followed by UV irradiation to initiate photo-cross-linking to nearby proteins. The labeled proteins were tagged with biotin via click chemistry with biotin azide and enriched by affinity chromatography with streptavidin. The eluted proteins were separated by SDS-PAGE, and Western blot analysis demonstrated that presenilin N-terminal fragment (PS1-NTF) was labeled by 53 (Figure 3). The labeling was deemed specific, because it was competed by pyridopyrazine-1,6-dione GSMs 52 and 54 (lanes 2 and 3). Despite the structural similarity to E2012-BPyne,^{16b} our data indicate that 53 binds differently to PS1-NTF because the labeling is not competed by 3 (lane 5). Furthermore, unlike E2012-BPyne, labeling by 53 in the presence of GSI L458 did not result in a dramatic increase in the labeling of PS1-NTF (lane 4).^{16b}

CONCLUSION

In summary, starting from our previously described amide series (i.e., 4 and 5), we have designed a novel series of GSMs. Our primary design objective was to identify a new heterocyclic

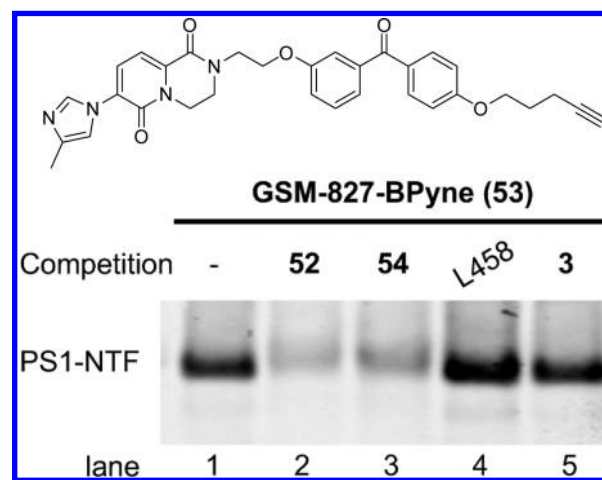


Figure 3. GSM-827-BPyne (53) specifically labels PS1-NTF in HeLa membranes. Photoaffinity labeling of 53 (5 μM, lanes 1–5) in HeLa membranes in the absence (lane 1) or presence of 50 μM GSM 52 (lane 2), 50 μM GSM 54³⁹ (lane 3), 1 μM GSI L458 (lane 4) or 50 μM 3 (lane 5), followed by click chemistry with biotin azide, streptavidin pull-down, and Western blot analysis with PS1-NTF antibody.

core as a replacement for the pyridyl amide moiety of 5, to improve physicochemical properties. We also sought to improve the alignment of potency and ADME parameters such as clearance, permeability, and MDR efflux ratio. These objectives were achieved through incorporation of conforma-

tional constraint, which ultimately led to the discovery of a novel GSM series containing a pyridopyrazine-1,6-dione bicyclic core. Within this series we have highlighted compounds that exhibit a 7-fold improvement in $A\beta$ -lowering activity in vitro as compared to reference compound **3** and possess significantly improved physicochemical properties. Lead compound **51** has good CNS-like physicochemical properties, as evidenced by improved CNS MPO and LipE relative to **3** (GSMs **51** and **3** have CNS MPO scores of 4.6 and 3.7, and LipE values of 3.9 and 2.3, respectively). This in turn translated into low clearance in vitro and in vivo, and excellent permeability and oral bioavailability. Robust in vivo efficacy was observed in a guinea pig model at 30 mg/kg, and reduction of brain $A\beta$ 42 was achieved in a dose-dependent manner. Of note is that this new GSM series successfully addresses the problems of CYP-inhibition and off-target activity that were observed with previous arylimidazole series. Our efforts also led to important insights into the GSM pharmacophore. By breaking the symmetry around the core and by locking rotamers through introduction of conformational constraint, we were able to establish directionality for the key polar interactions between heteroaryl-type γ -secretase modulators and the target binding site. Finally, chemical biology efforts involving design and synthesis of photoaffinity probe **53** demonstrated that the pyridinone class of GSMs binds to the N-terminal fragment of presenillin (PS1-NTF) within the of γ -secretase complex at a site that is distinct from that targeted by γ -secretase inhibitors. Additional efforts to further improve potency while maintaining the favorable physicochemical properties, ADME, and safety profiles of **50** and **51** will be disclosed in due course.

EXPERIMENTAL SECTION

General Methods. Solvents and reagents were of reagent grade and were used as supplied by the manufacturer. All reactions were run under a N_2 atmosphere. Organic extracts were routinely dried over anhydrous sodium sulfate or magnesium sulfate. Concentration refers to rotary evaporation under reduced pressure. Chromatography refers to flash chromatography using disposable RediSepR₄ 4 to 120 g silica columns or Biotage disposable columns on a CombiFlash Companion or Biotage horizon automatic purification system. Microwave reactions were carried out in a microwave reactor manufactured by Smithcreator of Personal Chemistry. 1H NMR spectra were recorded on Varian INOVA spectrometers (300, 400, or 500 MHz) (Varian Inc., Palo Alto, CA) at room temperature. Chemical shifts are expressed in parts per million δ relative to residual solvent as an internal reference. Peak multiplicities are expressed as follows: singlet (s), doublet (d), triplet (t), quartet (q), multiplet (m), and broad singlet (br s). HPLC purity analysis of final test compounds was carried out using one of the following three methods unless otherwise indicated. Method A: Compounds **46–49**, **52**, and **53**: liquid chromatography/photodiode array detector/evaporative light scattering detection coupled to single quadrupole mass spectrometry (LC/UV/ELSD/MS), Waters Atlantis dC18 4.6 \times 50 mm, 5 μ m; mobile phase A: 0.05% TFA in water (v/v); mobile phase B: 0.05% TFA in acetonitrile (v/v); gradient begins at 95.0% A, 5% B increasing to 5% A, 95% B over 4.0 min, hold at 5% A, 95% B until 5.0 min. Flow rate: 2 mL/min. Method B: Compounds **50** and **51**: UPLC/UV/MS using Waters CSH C18 2.1 \times 50 mm with 1.7 μ m particles; UV purity detected at 215 nm; mass spectrometer ESI positive negative switching acquiring from m/z 160 to 1000. Mobile phase A = 0.1% formic acid in water (v/v); mobile phase B = 0.1% formic acid in acetonitrile (v/v); gradient begins at 95% A, 5% B increasing to 100% B over 1.2 min, hold at 100% B until 1.5 min. Flow rate: 1.0 mL/min. Method C: Compounds **15**, **25b**, **27**, **28**, and **44**: UPLC/UV/MS. Mobile phase A: 0.05% TFA in water (v/v); mobile phase B: 0.05% TFA in acetonitrile (v/v); gradient begins at 95.0% A,

5% B increasing to 5% A, 95% B. All final test compounds were found to have purity >95% unless otherwise indicated.

N-(4-Fluoro-3-methoxybenzylidene)-2,2-dimethoxyethanamine (10). A solution of 4-fluoro-3-methoxybenzaldehyde (**9**) (7.00 g, 45.4 mmol) and 2,2-dimethoxyethanamine (5.88 mL, 54.5 mmol) in toluene (60 mL) was heated to reflux under a Dean–Stark trap for 1 h. The reaction mixture was allowed to cool to room temperature and concentrated under reduced pressure to provide the title compound (10.9 g, quantitative). LCMS m/z 242.2 ($M + 1$). 1H NMR (400 MHz, $CDCl_3$) δ 3.42 (s, 6H), 3.77 (dd, $J = 5.3, 1.2$ Hz, 2H), 3.94 (s, 3H), 4.68 (t, $J = 5.3$ Hz, 1H), 7.09 (dd, $J = 10.7, 8.4$ Hz, 1H), 7.16 (ddd, $J = 8.2, 4.7, 1.9$ Hz, 1H), 7.50 (dd, $J = 8.4, 1.9$ Hz, 1H), 8.21 (t, $J = 1.4$ Hz, 1H).

6-Fluoro-7-methoxyisoquinoline (12). Ethyl chloroformate (4.04 mL, 40.2 mmol) was added to a solution of N-(4-fluoro-3-methoxybenzylidene)-2,2-dimethoxyethanamine (**10**) (9.70 g, 40.2 mmol) in tetrahydrofuran (30 mL) at $-10^\circ C$. The reaction was stirred at $-10^\circ C$ for 5 min and then warmed to room temperature, whereupon trimethyl phosphite (6.05 mL, 48.2 mmol) was added. The reaction mixture was stirred at room temperature for 18 h and then concentrated under reduced pressure to provide ethyl 2,2-dimethoxyethyl[(dimethoxyphosphoryl)(4-fluoro-3-methoxyphenyl)methyl]carbamate (**11**) (17.0 g, quantitative), which was used in the subsequent step without purification. Intermediate **11** (2.41 g, 5.70 mmol) was treated with a 1.0 M solution of titanium tetrachloride in dichloromethane (34.2 mL, 34.2 mmol). The mixture was heated to reflux for 24 h, whereupon it was allowed to cool to room temperature and was poured into an aqueous solution of sodium hydroxide (1 M, 150 mL) and ethyl acetate (50 mL). The resulting white precipitate was removed by filtration, and the filtrate was extracted with ethyl acetate (2 \times 40 mL). The combined organic layers were dried (Na_2SO_4), filtered, and concentrated under reduced pressure. The resulting residue was purified by chromatography on silica gel (gradient: 0% to 10% methanol in ethyl acetate) to provide the title compound (573 mg, 57%). LCMS m/z 178.2 ($M + 1$). 1H NMR (400 MHz, $CDCl_3$) δ 4.03 (s, 3H), 7.31 (d, $J = 8.2$ Hz, 1H), 7.43 (d, $J = 11.3$ Hz, 1H), 7.53 (d, $J = 5.7$ Hz, 1H), 8.44 (d, $J = 5.9$ Hz, 1H), 9.12 (s, 1H).

6-Fluoro-7-methoxyisoquinoline 2-oxide (13). *m*-Chloroperoxybenzoic acid (1.57 g, 6.46 mmol) was added to a solution of 6-fluoro-7-methoxyisoquinoline (**12**) (573 mg, 3.23 mmol) in dichloromethane (20 mL). The mixture was stirred at room temperature for 3 h, whereupon it was poured into a mixture of aqueous sodium hydroxide solution (1 M, 50 mL) and 20% aqueous sodium thiosulfate solution (50 mL). The layers were separated, and the aqueous layer was extracted with dichloromethane (2 \times 25 mL). The combined organic layers were dried (Na_2SO_4), filtered, and concentrated under reduced pressure. The resulting residue was purified by chromatography on silica gel (gradient: 0% to 20% methanol in ethyl acetate) to provide the title compound (288 mg, 46%). LCMS m/z 193.9 ($M + 1$). 1H NMR (400 MHz, CD_3OD) δ 4.02 (s, 3H), 7.50 (d, $J = 8.2$ Hz, 1H), 7.65 (d, $J = 10.9$ Hz, 1H), 7.85 (d, $J = 7.0$ Hz, 1H), 8.10 (dd, $J = 7.0, 1.4$ Hz, 1H), 8.88 (s, 1H).

6-Fluoro-7-methoxyisoquinolin-1(2H)-one (14). 6-Fluoro-7-methoxyisoquinoline 2-oxide (**13**) (288 mg, 1.49 mmol) was dissolved in acetic anhydride (5.0 mL, 40 mmol) and heated to reflux for 3 h. The mixture was allowed to cool to room temperature and then was concentrated under reduced pressure. The resulting residue was treated with an aqueous solution of sodium hydroxide (2 M, 10 mL) and heated to $100^\circ C$ for 1 h. The mixture was cooled to room temperature and acidified to pH 6 with a 5% aqueous solution of citric acid. The resulting solid was isolated by filtration to provide the title compound (242 mg, 84%). LCMS m/z 193.9 ($M + 1$). 1H NMR (400 MHz, $CDCl_3$) δ 4.03 (s, 3H), 6.49 (d, $J = 7.2$ Hz, 1H), 7.11 (d, $J = 7.2$ Hz, 1H), 7.25 (d, $J = 11.5$ Hz, 1H), 7.92 (d, $J = 8.6$ Hz, 1H), 10.77 (br s, 1H).

2-(3-Chlorophenethyl)-6-fluoro-7-methoxyisoquinolin-1(2H)-one. Sodium hydride (60.2 mg, 60% dispersion in mineral oil, 1.50 mmol) was added to a solution of 6-fluoro-7-methoxyisoquinolin-1(2H)-one (**14**) (242 mg, 1.25 mmol) in *N,N*-dimethylacetamide (10

mL). The mixture was stirred at room temperature for 1 h and then treated with 1-(2-bromoethyl)-3-chlorobenzene (0.22 mL, 1.50 mmol). After being stirred for 18 h, the reaction was judged incomplete by TLC. Additional sodium hydride (30 mg, 60% dispersion in mineral oil, 0.75 mmol) and 1-(2-bromoethyl)-3-chlorobenzene (0.200 mL, 1.36 mmol) were added to the mixture. The reaction was stirred at room temperature for 24 h, whereupon it was poured into water (40 mL) and extracted with dichloromethane (3 × 25 mL). The combined organic layers were dried (Na₂SO₄), filtered, and concentrated under reduced pressure. The resulting residue was purified by chromatography on silica gel (gradient: 0% to 50% ethyl acetate in heptane) to provide the title compound (259 mg, 62%). LCMS *m/z* 332.2 (M + 1). ¹H NMR (400 MHz, CDCl₃) δ 3.05–3.11 (m, 2H), 4.02 (s, 3H), 4.17–4.23 (m, 2H), 6.32 (d, *J* = 7.4 Hz, 1H), 6.77 (d, *J* = 7.4 Hz, 1H), 7.05–7.10 (m, 1H), 7.18 (d, *J* = 11.3 Hz, 1H), 7.20–7.25 (m, 3H), 7.96 (d, *J* = 8.6 Hz, 1H).

2-(3-Chlorophenethyl)-7-methoxy-6-(4-methyl-1H-imidazol-1-yl)isoquinolin-1(2H)-one (15). 4-Methylimidazole (126 mg, 1.54 mmol) and potassium carbonate (425 mg, 3.08 mmol) were added to a solution of 2-(3-chlorophenethyl)-6-fluoro-7-methoxyisoquinolin-1(2H)-one (255 mg, 0.769 mmol) in dimethyl sulfoxide (5 mL). The mixture was heated to 135 °C for 14 h, whereupon it was cooled to room temperature and poured into water (20 mL). The aqueous mixture was extracted with dichloromethane (3 × 30 mL), and the combined organic layers were dried (Na₂SO₄), filtered, and concentrated under reduced pressure. The resulting residue was purified by silica gel chromatography (gradient: 0% to 6% [2 M ammonia in methanol] in ethyl acetate) to provide a 2.5:1 mixture of imidazole regioisomers (160 mg, 53%). This mixture was further purified by HPLC (Phenomenex Luna (2) C₁₈, 21.2 × 150 mm, 5 μm; 0.1% formic acid modifier, 95% water/5% acetonitrile, linear gradient to 5% water/95% acetonitrile over 10.0 min, then 100% acetonitrile for 1.0 min; flow rate: 28 mL/min) to provide the title compound (20 mg, 7%). LCMS *m/z* 394.2 (M + 1). ¹H NMR (400 MHz, CDCl₃) δ 2.29–2.34 (m, 3H), 3.08 (t, *J* = 7.3 Hz, 2H), 4.01 (s, 3H), 4.18–4.25 (m, 2H), 6.36 (d, *J* = 7.4 Hz, 1H), 6.78 (d, *J* = 7.2 Hz, 1H), 7.03 (t, *J* = 1.0 Hz, 1H), 7.04–7.10 (m, 1H), 7.19–7.24 (m, 3H), 7.39 (s, 1H), 7.83 (d, *J* = 1.2 Hz, 1H), 8.01 (s, 1H). HPLC purity >95%.

(E)-3-(3-Bromo-2-methoxyphenyl)acrylic Acid (18). To a solution of 3-bromo-2-methoxybenzaldehyde (16) (7.42 g, 34.5 mmol) in pyridine (25.1 mL) was added malonic acid (5.50 g, 51.8 mmol) followed by piperidine (1.06 mL, 10.4 mmol). The reaction mixture was heated to 120 °C for 6 h, whereupon it was allowed to cool to room temperature and acidified to pH < 3 using concentrated hydrochloric acid. The resulting solid was collected by filtration, and the residue was purified via chromatography on silica gel (5% [2 M acetic acid in ethyl acetate] in heptane) to provide the title compound (4.43 g, 50%). LCMS *m/z* 254.1 (M – 1). ¹H NMR (400 MHz, CD₃OD) δ 3.83 (s, 3H), 6.56 (d, *J* = 16.0 Hz, 1H), 7.09 (t, *J* = 8.0 Hz, 1H), 7.67 (dd, *J* = 1.6, 7.8 Hz, 1H), 7.64 (dd, *J* = 1.6, 8.0 Hz, 1H), 7.91 (d, *J* = 16.2 Hz, 1H).

(E)-3-(3-Fluoro-2-methoxyphenyl)acrylic Acid (19). A solution of 3-fluoro-2-methoxybenzaldehyde (17) (16.1 g, 104 mmol) and malonic acid (16.6 g, 157 mmol) in pyridine (51 mL) and piperidine (3.2 mL) was heated to 120 °C for 6 h. The reaction was allowed to cool to room temperature, and concentrated aqueous hydrochloric acid was added to reach pH < 3. The resulting precipitate was collected via filtration, washed with water, and recrystallized from ethyl acetate to provide the title compound as a solid (3.84 g, 19%). LCMS *m/z* 195.3 (M-1). ¹H NMR (400 MHz, CD₃OD) δ 3.95 (d, *J* = 1.9 Hz, 3H), 6.54 (d, *J* = 16.0 Hz, 1H), 7.09 (ddd, *J* = 8.2, 8.0, 5.1 Hz, 1H), 7.18 (ddd, *J* = 11.5, 8.2, 1.6 Hz, 1H), 7.44 (br d, *J* = 7.8 Hz, 1H), 7.92 (d, *J* = 16.2 Hz, 1H).

(E)-3-(3-Fluoro-2-methoxyphenyl)acryloyl Azide (21). A mixture of (E)-3-(3-fluoro-2-methoxyphenyl)acrylic acid (19) (889 mg, 4.53 mmol) in thionyl chloride (3.3 mL, 45.3 mmol) was stirred at room temperature for 16 h and then heated to reflux for 2 h. The volatiles were evaporated under reduced pressure, and the crude material was azeotroped with toluene. The resulting residue (973 mg) was dissolved in acetone (3.2 mL) and cooled to 0 °C. A solution of sodium azide

(383 mg, 5.9 mmol) in water (1.2 mL) was added, the cold bath was removed, and the reaction was stirred at room temperature for 2 h. The reaction mixture was poured into diethyl ether (30 mL) and water (30 mL), and the layers were separated. The aqueous layer was extracted with ether (2 × 30 mL), and the combined organic layers were dried (Na₂SO₄), filtered, and concentrated under reduced pressure to provide the title compound (996 mg, 99%). ¹H NMR (400 MHz, CDCl₃) δ 4.00 (d, *J* = 2.3 Hz, 3H), 6.51 (d, *J* = 16.0 Hz, 1H), 6.99–7.07 (m, 1H), 7.15 (ddd, *J* = 11.5, 8.2, 1.6 Hz, 1H), 7.31 (d, *J* = 7.8 Hz, 1H), 8.01 (d, *J* = 16.0 Hz, 1H).

6-Bromo-5-methoxyisoquinolin-1(2H)-one (22). Thionyl chloride (2.5 mL, 34 mmol) was added to a round-bottom flask charged with (E)-3-(3-bromo-2-methoxyphenyl)acrylic acid (18) (0.88 g, 3.4 mmol). The reaction mixture was stirred for 16 h at room temperature followed by heating at 90 °C for 2 h. The reaction was then allowed to cool to room temperature, and the volatiles were removed under reduced pressure. After azeotroping with toluene, the resulting residue (0.95 g) was dissolved in acetone (3.2 mL) and cooled to 0 °C. Sodium azide (0.34 g, 5.3 mmol) in water (1.2 mL) was added, and the reaction mixture was stirred at room temperature for 2 h. Diethyl ether (30 mL) and water (30 mL) were added, and the layers were separated. The aqueous layer was extracted with diethyl ether (2 × 30 mL), the combined organic layers were dried (Na₂SO₄) and filtered, and the solvent was removed under reduced pressure. The resulting residue (0.89 g) was dissolved in 1,2-dichlorobenzene (20 mL) and subsequently heated to 140 °C. After 1 h, when gas evolution had subsided, catalytic iodine was added to the reaction mixture and the temperature was increased to 185 °C for an additional 1.5 h. The reaction mixture was allowed to cool to room temperature, the solvent was partially removed, and the material was isolated through crystallization to afford the desired product (0.44 g, 51%). LCMS *m/z* 255.9 (M + 1). ¹H NMR (400 MHz, CDCl₃) δ 3.95 (s, 3H), 6.83 (d, *J* = 7.2 Hz, 1H), 7.22 (d, *J* = 7.6 Hz, 1H), 7.66 (d, *J* = 8.6 Hz, 1H), 8.06 (d, *J* = 8.6 Hz, 1H), 11.2 (br s, 1H).

6-Fluoro-5-methoxyisoquinolin-1(2H)-one (23). A solution of (E)-3-(3-fluoro-2-methoxyphenyl)acryloyl azide (21) (996 mg, 4.50 mmol) in 1,2-dichlorobenzene (30 mL) was heated to 140 °C for 1 h until gas formation subsided. Catalytic iodine was added, and the temperature was increased to 185 °C. The reaction mixture was heated to 185 °C for 4 days, whereupon it was allowed to cool to room temperature. The reaction was concentrated under reduced pressure, and the residue was purified via chromatography on silica gel (gradient: 0% to 10% ethyl acetate in heptane, then 0% to 10% [10% methanol in ethyl acetate] in heptane). The resulting residue (469 mg) was purified further by prep-HPLC (Gemini 50 × 100 mm C18; mobile phase A: 0.1% formic acid in water; mobile phase B: acetonitrile; gradient: 25% to 75% B; flow rate: 75 mL/min) to afford the title compound (143 mg, 16%) as a solid. LCMS *m/z* 194.3 (M + 1). ¹H NMR (400 MHz, CD₃OD) δ 4.06 (d, *J* = 1.9 Hz, 3H), 6.87 (d, *J* = 7.4 Hz, 1H), 7.14 (d, *J* = 6.6 Hz, 1H), 7.24 (dd, *J* = 11.1, 9.0 Hz, 1H), 8.08–8.19 (m, 1H), 10.28 (br s, 1H).

6-Bromo-2-(3-chlorophenethyl)-5-methoxyisoquinolin-1(2H)-one (24). Sodium hydride (60% dispersion in mineral oil, 0.61 g, 15.3 mmol) was added to a solution of 6-bromo-5-methoxyisoquinolin-1(2H)-one (22) (0.44 g, 1.7 mmol) in dimethylacetamide (20.0 mL), and the reaction mixture was stirred at room temperature for 1 h. 1-(2-Bromoethyl)-3-chlorobenzene (2.25 mL, 15.3 mmol) was added, and stirring was continued for 48 h. Additional sodium hydride (0.70 g, 17.6 mmol) and 1-(2-bromoethyl)-3-chlorobenzene (2.00 mL, 13.6 mmol) were added, and the reaction mixture was stirred for an additional 24 h, whereupon it was poured into water (40 mL) and ethyl acetate (30 mL). The layers were separated, and the aqueous layer was extracted twice with diethyl ether. The combined organic layers were dried (Na₂SO₄), filtered, and concentrated under reduced pressure. The resulting residue was purified via chromatography on silica gel (gradient: 0% to 50% ethyl acetate in heptane) to provide the desired product (0.30 g, 45%). LCMS *m/z* 393.8 (M + 1). ¹H NMR (400 MHz, CDCl₃) δ 3.07 (m, 2H), 3.92 (s, 3H), 4.18 (m, 2H), 6.63 (d, *J* = 7.6 Hz, 1H), 6.84 (d, *J* = 7.4 Hz, 1H), 7.08–7.06 (m, 1H), 7.22–7.20 (m, 3H), 7.63 (d, *J* = 8.6 Hz, 1H), 8.08 (d, *J* = 8.6, 1H).

2-(3-Chlorophenethyl)-5-methoxy-6-(4-methyl-1H-imidazol-1-yl)isoquinolin-1(2H)-one (25b). Cesium carbonate (0.16 g, 0.48 mmol) and 4-methylimidazole (30 mg, 0.36 mmol) were added to a solution of 6-bromo-2-(3-chlorophenethyl)-5-methoxyisoquinolin-1(2H)-one (24) (0.10 g, 0.24 mmol) in *N,N*-dimethylformamide (2.0 mL). Nitrogen was gently bubbled through the reaction mixture for 5 min, and copper(I) iodide (20 mg, 0.12 mmol) was added. Nitrogen was bubbled through the reaction mixture for an additional 30 min, and the reaction was then heated to 100 °C. After stirring the reaction at 100 °C for 3 days, it was allowed to cool to room temperature and filtered through Celite. The filtrate was concentrated under reduced pressure, and the residue was purified via reversed phase prep-HPLC (gradient: 5% to 15% acetonitrile in water containing 0.1% formic acid) to provide the desired product (20 mg, 20%). LCMS *m/z* 394.5 (*M* + 1). ¹H NMR (400 MHz, CDCl₃) δ 2.33 (s, 3H), 3.09 (m, 2H), 3.55 (s, 3H), 4.21 (m, 2H), 6.70 (d, *J* = 7.4 Hz, 1H), 6.88 (*J* = 7.6 Hz, 1H), 7.07–7.24 (m, 7H), 7.40 (d, *J* = 8.6 Hz, 1H). HPLC purity: 93%.

6-Fluoro-5-methoxy-2-[3-(trifluoromethyl)benzyl]isoquinolin-1(2H)-one (26). Sodium hydride (60% dispersion in mineral oil, 44.4 mg, 1.11 mmol) was added to a solution of 6-fluoro-5-methoxyisoquinolin-1(2H)-one (23) (143 mg, 0.74 mmol) in *N,N*-dimethylformamide (5 mL). The mixture was stirred at room temperature for 1 h, whereupon 3-(trifluoromethyl)benzyl bromide (212 mg, 0.89 mmol) was added. The reaction mixture was stirred at room temperature overnight, whereupon it was poured into ethyl acetate (10 mL) and water (30 mL). The layers were separated, and the aqueous layer was extracted with ethyl acetate (2 × 10 mL). The combined organic layers were dried (Na₂SO₄), filtered, and concentrated under reduced pressure. The resulting residue was purified by chromatography on silica gel (gradient: 0% to 40% ethyl acetate in heptane) to afford the title compound as a solid (253 mg, 97%). LCMS *m/z* 352.5 (*M* + 1). ¹H NMR (400 MHz, CD₃OD) δ 4.01 (s, 3H), 5.20 (s, 2H), 6.80 (d, *J* = 7.6 Hz, 1H), 7.08 (d, *J* = 7.6 Hz, 1H), 7.14–7.26 (m, 1H), 7.37–7.57 (m, 4H), 8.11 (dd, *J* = 9.0, 4.9 Hz, 1H).

5-Hydroxy-6-(4-methyl-1H-imidazol-1-yl)-2-[3-(trifluoromethyl)benzyl]isoquinolin-1(2H)-one (27). A mixture of 6-fluoro-5-methoxy-2-[3-(trifluoromethyl)benzyl]isoquinolin-1(2H)-one (26) (253 mg, 0.72 mmol), 4-methylimidazole (118 mg, 1.44 mmol), and potassium carbonate (398 mg, 2.88 mmol) in *N,N*-dimethylformamide (5 mL) was stirred at 100 °C for 3 days and then at 120 °C for 12 h. The reaction was allowed to cool to room temperature and filtered, the solids were washed with acetonitrile, and the combined filtrate and washings were concentrated under reduced pressure. The resulting residue was purified by prep-HPLC (column: Gemini 50 × 100 mm C18 (acidic or basic, >150 mg), injection volume: 900 μL × 7; solvent A: 0.1% formic acid in water; solvent B: acetonitrile; gradient 30% to 80% B; collection time: 3–10 min; flow rate: 75 mL/min; wavelength 220 nm) to afford the desired product as a mixture containing the imidazole regioisomer side product (142 mg). The regioisomers were further separated by SFC prep-HPLC (column: Chiralcel OD-H (4.6 mm × 25 cm); mobile phase 25% methanol in carbon dioxide; flow rate: 2.5 mL/min) to afford the title compound as a solid (80 mg, 27%). LCMS *m/z* 400.5 (*M* + 1). ¹H NMR (400 MHz, CD₃OD) δ 2.30 (s, 3H), 5.35 (s, 2H), 7.10 (dd, *J* = 7.6, 0.8 Hz, 1H), 7.23 (t, *J* = 1.2 Hz, 1H), 7.46 (d, *J* = 8.6 Hz, 1H), 7.50–7.60 (m, 2H), 7.60–7.66 (m, 2H), 7.68 (s, 1H), 7.95 (d, *J* = 8.6 Hz, 1H), 8.05 (d, *J* = 1.4 Hz, 1H). HPLC purity >95%.

5-Hydroxy-6-(4-methyl-1H-imidazol-1-yl)-2-[3-(trifluoromethyl)benzyl]-3,4-dihydroisoquinolin-1(2H)-one (28). 5-Hydroxy-6-(4-methyl-1H-imidazol-1-yl)-2-[3-(trifluoromethyl)benzyl]isoquinolin-1(2H)-one (27) (30 mg, 0.075 mmol) in 20 mL of methanol was subjected to H-Cube hydrogenation (10% Pd/C, 50 bar, 60 °C, 0.4 mL/min). The solvent was evaporated under reduced pressure to afford the title compound as an oil (29 mg, 97%). LCMS *m/z* 402.6 (*M* + 1). ¹H NMR (400 MHz, CD₃OD) δ 2.07 (s, 3H), 3.08 (t, *J* = 6.7 Hz, 2H), 3.52 (t, *J* = 6.7 Hz, 2H), 4.85 (s, 2H), 6.79 (s, 1H), 7.08 (d, *J* = 8.2 Hz, 1H), 7.36–7.42 (m, 1H), 7.48 (d, *J* = 7.2 Hz, 1H), 7.51–7.64 (m, 3H), 7.69 (d, *J* = 8.2 Hz, 1H). HPLC purity >95%.

5-(4-Methyl-1H-imidazol-1-yl)-6-oxo-1,6-dihydropyridine-2-carboxylic Acid, Hydrobromide Salt (34). A solution of methyl 6-methoxy-5-(4-methyl-1H-imidazol-1-yl)pyridine-2-carboxylate³⁴ (33) (3.82 g, 15.9 mmol) in acetic acid (30 mL) and aqueous hydrobromic acid (48%, 30 mL) was heated to reflux for 4 h. The reaction was allowed to cool to room temperature and then cooled further to 0 °C using an ice–water bath. The resulting precipitate was collected via filtration and washed with ice–water (30 mL). Recrystallization from ethanol (20 mL) provided the title compound as a light yellow solid (3.79 g, 79%). LCMS *m/z* 220.1 (*M* + 1). ¹H NMR (400 MHz, DMSO-*d*₆) δ 2.34 (br s, 3H), 7.09 (d, *J* = 7.4 Hz, 1H), 7.88–7.91 (m, 1H), 8.07 (d, *J* = 7.6 Hz, 1H), 9.58–9.60 (m, 1H), 12.6 (br s, 1H).

5-(4-Methyl-1H-imidazol-1-yl)-6-oxo-1,6-dihydropyridine-2-carboxylic Acid, Hydrochloride Salt (35). A solution of methyl 6-methoxy-5-(4-methyl-1H-imidazol-1-yl)pyridine-2-carboxylate³⁴ (33) (34.3 g, 139 mmol) in aqueous hydrochloric acid (37%, 230 mL) and 1,4-dioxane (230 mL) was heated to reflux for 18 h, whereupon it was allowed to cool to room temperature. The reaction was filtered, and the solids were washed with 1,4-dioxane (2 × 100 mL). The solids were mixed with methanol (500 mL), and the volatiles were removed under reduced pressure. The residue was stirred with methanol (100 mL) for 15 min, and 1,4-dioxane (250 mL) was added. The resulting mixture was stirred for 15 min, whereupon the solids were collected by filtration and washed with 1,4-dioxane to provide the title compound as a beige solid (35.4 g, 99%). LCMS *m/z* 220.1 (*M* + 1). ¹H NMR (300 MHz, DMSO-*d*₆) δ 2.33 (d, *J* = 0.9 Hz, 3H), 7.09 (d, *J* = 7.5 Hz, 1H), 7.84–7.87 (m, 1H), 8.04 (d, *J* = 7.5 Hz, 1H), 9.50 (d, *J* = 1.6 Hz, 1H).

2-(2-Chloroethyl)-7-(4-methyl-1H-imidazol-1-yl)-3,4-dihydro-2H-pyrido[1,2-*a*]pyrazine-1,6-dione (41). Potassium carbonate (195.4 g, 1414 mmol) was added to a mixture of 5-(4-methyl-1H-imidazol-1-yl)-6-oxo-1,6-dihydropyridine-2-carboxylic acid, hydrochloride salt (35) (34.5 g, 135 mmol) and bis(2-chloroethyl)amine hydrochloride (40) (37.8 g, 212 mmol) in *N,N*-dimethylformamide (670 mL), and the reaction was stirred for 10 min. HATU (83.5 g, 219 mmol) was added, and stirring was continued for an additional 3 h and 40 min. The reaction mixture was poured into water (4 L), stirred for 30 min, and then extracted with dichloromethane (3 × 1 L). The combined organic layers were washed with saturated aqueous sodium chloride solution (3 × 3 L), dried (MgSO₄), filtered, and concentrated under reduced pressure. The residue was stirred in ethyl acetate (approximately 50 mL) for 30 min, whereupon the solids were collected by filtration and washed with ethyl acetate and pentane to provide the title compound as a yellow solid (23.0 g, 56%). LCMS *m/z* 307.1 (*M* + 1). ¹H NMR (300 MHz, CDCl₃) δ 2.29 (br s, 3H), 3.80–3.93 (m, 6H), 4.38–4.44 (m, 2H), 7.13–7.16 (m, 1H), 7.27 (d, *J* = 7.6 Hz, 1H), 7.45 (d, *J* = 7.6 Hz, 1H), 8.24 (d, *J* = 1.0 Hz, 1H).

2-[3-(Trifluoromethyl)benzyl]-7-(4-methyl-1H-imidazol-1-yl)-3,4-dihydro-2H-pyrido[1,2-*a*]pyrazine-1,6-dione (44). To a solution of 5-(4-methyl-1H-imidazol-1-yl)-6-oxo-1,6-dihydropyridine-2-carboxylic acid, hydrochloride salt (35) (68 mg, 0.20 mmol) in *N,N*-dimethylformamide (6.0 mL) was added HATU (140 mg, 0.36 mmol), *N,N*-diisopropylethylamine (0.30 mL, 2.0 mmol), and finally [2-(3-(trifluoromethyl)benzylamino)ethanol (50 mg, 0.23 mmol). The reaction mixture was stirred at room temperature for 14 h, whereupon additional HATU (102 mg, 0.26 mmol) was added. Stirring was continued for 4 h, and the reaction mixture was poured into saturated aqueous sodium bicarbonate solution (50 mL) and washed with ethyl acetate (2 × 50 mL). The combined organic layers were washed with saturated aqueous sodium chloride solution (2 × 50 mL), dried (NaSO₄), filtered, and concentrated under reduced pressure. The resulting residue was purified via chromatography on silica gel (gradient: 10% to 100% ethyl acetate in heptane) to afford the title compound as a tan solid (20 mg, 23%). LCMS *m/z* 403.1 (*M* + 1). ¹H NMR (400 MHz, CDCl₃) δ 2.25 (d, *J* = 1.0 Hz, 3H), 3.59 (dd, *J* = 6.5, 5.2 Hz, 2H), 4.29 (dd, *J* = 6.5, 5.2 Hz, 2H), 4.80 (s, 2H), 7.10 (t, *J* = 1.2 Hz, 1H), 7.31 (d, *J* = 7.6 Hz, 1H), 7.43 (d, *J* = 7.6 Hz, 1H), 7.47–7.51 (m, 2H), 7.52–7.60 (m, 2H), 8.19 (d, *J* = 1.2 Hz, 1H). HPLC purity >95%.

2-(*tert*-Butyldimethylsilyloxy)-*N*-[1-(4-chlorophenyl)cyclopropyl]-methylethanamine. A solution of [1-(4-chlorophenyl)cyclopropyl]-methanamine (10.0 mg, 0.055 mmol) and (*tert*-butyldimethylsilyloxy)-acetaldehyde (9.3 mg, 0.053 mmol) in dichloroethane (17.0 mL) was stirred for 5 min at room temperature, whereupon sodium triacetoxyborohydride (15.0 mg, 0.071 mmol) was added. The mixture was stirred at room temperature for 18 h and then poured into a saturated aqueous solution of sodium bicarbonate (50 mL) and washed with dichloromethane (2 × 20 mL). The combined organic layers were washed with brine (2 × 50 mL), dried (Na₂SO₄), filtered, and concentrated under reduced pressure to afford the title compound (20 mg, LCMS *m/z* 340.2 (M + 1) which was used directly in the next without further purification.

2-[1-(4-Chlorophenyl)cyclopropyl]methylaminoethanol. A solution of 0.4 M HCl in methanol at 0 °C (0.5 mL, 0.2 mmol) was added to a solution of 2-(*tert*-butyldimethylsilyloxy)-*N*-[1-(4-chlorophenyl)cyclopropyl]methyl]ethanamine (20 mg, 0.059 mmol) in methanol (0.5 mL). The reaction was stirred at room temperature for 64 h, whereupon it was poured into a saturated solution of aqueous sodium bicarbonate (50 mL) and washed with ethyl acetate (50 mL). The layers were separated, and the organic layer was washed with brine (2 × 50 mL), dried (Na₂SO₄), filtered, and concentrated under reduced pressure. The residue was purified by chromatography on silica gel (gradient: 10% to 100% ethyl acetate in heptane) to afford the title compound as a clear colorless oil (13 mg, quant.). LCMS *m/z* 226.2 (M + 1).

2-[1-(4-Chlorophenyl)cyclopropyl]methyl]-7-(4-methyl-1*H*-imidazol-1-yl)-3,4-dihydro-2*H*-pyrido[1,2-*a*]pyrazine-1,6-dione, Tri-fluoroacetate Salt (**45**). To a solution of 5-(4-methyl-1*H*-imidazol-1-yl)-6-oxo-1,6-dihydropyridine-2-carboxylic acid, hydrobromide salt (**34**) (22 mg, 0.06 mmol) and 2-[1-(4-chlorophenyl)cyclopropyl]methylaminoethanol (13 mg, 0.06 mmol) in *N,N*-dimethylformamide (1.5 mL) were added HATU (50 mg, 0.13 mmol) and *N,N*-diisopropylethylamine (0.30 mL, 2.0 mmol). The reaction mixture was stirred at room temperature for 17 h, whereupon it was partitioned between dichloromethane and water. The aqueous layer was extracted with dichloromethane, and the combined organic layers were dried (Na₂SO₄), filtered through silica gel, and concentrated under reduced pressure. The residue was dissolved in dimethyl sulfoxide (1 mL) and purified by reversed-phase HPLC Column: Waters Sunfire C18 19 × 100, 5 μm; mobile phase A: 0.05% TFA in water (v/v); mobile phase B: 0.05% TFA in acetonitrile (v/v); gradient: 85.0% water/15.0% acetonitrile linear to 0% water/100% acetonitrile in 8.5 min, hold at 0% water/100% acetonitrile to 10.0 min. Flow rate: 25 mL/min. Purity was determined using liquid chromatography/photodiode array detector/evaporative light scattering detection coupled to single quadrupole mass spectrometry (LC/UV/ELSD/MS) using these standard conditions: Waters Atlantis dC₁₈ columns, 6 × 50 mm, 5 μm, at 2 mL/min flow rate; mobile phase A 0.05% trifluoroacetic acid in water (v/v); mobile phase B 0.05% trifluoroacetic acid in acetonitrile (v/v); 95% water/5% acetonitrile to 5% water/95% acetonitrile linear gradient over 4 min, and holding at final gradient for an additional 1 min. Retention time: 2.4 min. LCMS *m/z* 409.2 (M + 1). ¹H NMR (400 MHz, CDCl₃) δ 8.26 (d, *J* = 1.2 Hz, 1H), 7.42 (d, *J* = 7.8 Hz, 1H), 7.31–7.22 (m, 4H), 7.17 (d, *J* = 7.8 Hz, 1H), 7.10 (s, 1H), 4.08–4.02 (m, 2H), 3.74 (s, 2H), 3.38–3.32 (m, 2H), 2.26 (d, *J* = 0.8 Hz, 3H), 1.04–0.99 (m, 2H), 0.95–0.91 (m, 2H). HPLC purity >95%.

Parallel Medicinal Chemistry Protocol for Preparation of 2-[2-(Aryloxy)ethyl]- and 2-[2-(heteroaryloxy)ethyl]-7-(4-methyl-1*H*-imidazol-1-yl)-3,4-dihydro-2*H*-pyrido[1,2-*a*]pyrazine-1,6-diones **46–49 and **52**.** 2-(2-Chloroethyl)-7-(4-methyl-1*H*-imidazol-1-yl)-3,4-dihydro-2*H*-pyrido[1,2-*a*]pyrazine-1,6-dione (**41**) (20–35 mg) and a suitably substituted phenol (1–1.5 equiv) were combined in dimethyl sulfoxide (1.0 mL). After addition of potassium carbonate (3.5 equiv), the reaction mixture was heated at 100 °C until the reaction was judged to be complete via LCMS analysis (generally 1 to 3 h). The mixture was allowed to cool to room temperature and filtered, and the filtrate was purified using reversed phase HPLC with an appropriate gradient using the following system: Column: Waters Sunfire C18 19

× 100, 5 μm; mobile phase A: 0.05% trifluoroacetic acid in water (v/v); mobile phase B: 0.05% trifluoroacetic acid in acetonitrile (v/v). Flow rate: 25 mL/min.

7-(4-Methyl-1*H*-imidazol-1-yl)-2-[2-(trifluoromethyl)phenoxy]ethyl]-3,4-dihydro-1*H*-pyrido[1,2-*a*]pyrazine-1,6(2*H*)-dione (**46**). LCMS *m/z* 433.1 (M + 1). ¹H NMR (600 MHz, DMSO-*d*₆) δ 9.25 (s, 1H), 8.01 (d, *J* = 7.9 Hz, 1H), 7.76 (s, 1H), 7.67–7.57 (m, 2H), 7.31 (d, *J* = 8.3 Hz, 1H), 7.19–7.14 (m, 1H), 7.11 (t, *J* = 7.5 Hz, 1H), 4.35 (t, *J* = 5.0 Hz, 2H), 4.28–4.24 (m, 2H), 3.93 (t, *J* = 5.3 Hz, 2H), 3.86–3.82 (m, 2H), 2.30 (s, 3H). HPLC purity >95%.

2-[2-(2-Chlorophenoxy)ethyl]-7-(4-methyl-1*H*-imidazol-1-yl)-3,4-dihydro-1*H*-pyrido[1,2-*a*]pyrazine-1,6(2*H*)-dione (**47**). LCMS *m/z* 399.1 (M + 1). ¹H NMR (600 MHz, DMSO-*d*₆) δ 9.24 (s, 1H), 8.01 (d, *J* = 7.5 Hz, 1H), 7.75 (s, 1H), 7.42 (d, *J* = 7.9 Hz, 1H), 7.33–7.28 (m, 1H), 7.20–7.15 (m, 2H), 6.97 (t, *J* = 7.7 Hz, 1H), 4.30–4.28 (m, 4H), 3.94–3.92 (m, 4H), 2.30 (s, 3H). HPLC purity >95%.

7-(4-Methyl-1*H*-imidazol-1-yl)-2-[2-[3-(trifluoromethyl)phenoxy]ethyl]-3,4-dihydro-1*H*-pyrido[1,2-*a*]pyrazine-1,6(2*H*)-dione (**48**). LCMS *m/z* 433.1 (M + 1). ¹H NMR (600 MHz, DMSO-*d*₆) δ 9.21 (br s, 1H), 8.00 (d, *J* = 7.9 Hz, 1H), 7.74 (s, 1H), 7.56–7.49 (m, 1H), 7.32–7.26 (m, 2H), 7.16 (d, *J* = 7.5 Hz, 1H), 4.30 (t, *J* = 5.5 Hz, 2H), 4.28–4.23 (m, 2H), 3.91 (t, *J* = 5.3 Hz, 2H), 3.89–3.86 (m, 2H), 2.30 (s, 3H). HPLC purity >95%.

7-(4-Methyl-1*H*-imidazol-1-yl)-2-[2-[4-(trifluoromethyl)phenoxy]ethyl]-3,4-dihydro-1*H*-pyrido[1,2-*a*]pyrazine-1,6(2*H*)-dione (**49**). LCMS *m/z* 433.1 (M + 1). ¹H NMR (600 MHz, DMSO-*d*₆) δ 9.43 (s, 1H), 8.05 (dd, *J* = 7.7, 2.0 Hz, 1H), 7.82 (s, 1H), 7.66 (d, *J* = 7.0 Hz, 2H), 7.12–7.20 (m, 3H), 4.24–4.34 (m, 4H), 3.85–3.94 (m, 4H), 2.33 (s, 3H). HPLC purity >95%.

2-[2-(7-Fluoronaphthalen-1-yloxy)ethyl]-7-(4-methyl-1*H*-imidazol-1-yl)-3,4-dihydro-1*H*-pyrido[1,2-*a*]pyrazine-1,6(2*H*)-dione (**52**). LCMS *m/z* 433.3 (M + 1). ¹H NMR (400 MHz, CDCl₃) δ 8.20 (s, 1H), 7.79 (dd, *J* = 5.5, 9.0 Hz, 1H), 7.69 (dd, *J* = 2.5, 10.4 Hz, 1H), 7.46–7.38 (m, 2H), 7.32 (t, *J* = 7.9 Hz, 1H), 7.29–7.22 (m, 2H), 7.10 (s, 1H), 6.83 (d, *J* = 7.6 Hz, 1H), 4.42 (t, *J* = 4.8 Hz, 2H), 4.40–4.34 (m, 2H), 4.11 (t, *J* = 4.8 Hz, 2H), 4.00–3.94 (m, 2H), 2.26 (s, 3H). HPLC purity >95%.

1-(2-Bromoethoxy)-4-fluoro-2-(trifluoromethyl)benzene. A mixture of 4-fluoro-2-(trifluoromethyl)phenol (1.05 g, 5.83 mmol), 2-bromoethanol (0.62 mL, 8.7 mmol), and triphenylphosphine (2.29 g, 8.73 mmol) in tetrahydrofuran (20 mL) was stirred for 5 min. Diisopropyl azodicarboxylate (94%, 1.84 mL, 8.71 mmol) was added dropwise over 20 min, and the reaction was stirred at room temperature for 16 h. Water (50 mL) was added, and the mixture was extracted with dichloromethane (2 × 75 mL). The combined organic layers were washed with saturated aqueous sodium chloride solution (50 mL), dried (MgSO₄), filtered, and concentrated under reduced pressure. Purification via chromatography on silica gel (gradient: 0% to 10% ethyl acetate in heptane) afforded the title compound as a white solid (600 mg, 36%). GCMS *m/z* 286. ¹H NMR (400 MHz, CDCl₃) δ 3.66 (dd, *J* = 6.6, 6.4 Hz, 2H), 4.35 (dd, *J* = 6.5, 6.4 Hz, 2H), 6.97 (br dd, *J* = 9.0, 4.1 Hz, 1H), 7.18–7.24 (m, 1H), 7.32 (br dd, *J* = 8.3, 3.2 Hz, 1H).

2-[2-[4-Fluoro-2-(trifluoromethyl)phenoxy]ethyl]aminoethanol. A mixture of 1-(2-bromoethoxy)-4-fluoro-2-(trifluoromethyl)benzene (600 mg, 2.09 mmol) and 2-aminoethanol (2.20 mL, 52.4 mmol) was heated to 80 °C for 1.5 h. The reaction was allowed to cool to room temperature, diluted with ethyl acetate (75 mL), and washed with aqueous sodium hydroxide solution (1 N, 4 × 50 mL). The organic layer was dried (MgSO₄), filtered, and concentrated under reduced pressure to provide the title compound as a white solid (550 mg, 99%). LCMS *m/z* 268.1 (M + 1). ¹H NMR (400 MHz, CD₃OD) δ 2.80 (br dd, *J* = 5.5, 5.4 Hz, 2H), 3.04 (dd, *J* = 5.4, 5.2 Hz, 2H), 3.68 (br dd, *J* = 5.6, 5.4 Hz, 2H), 4.20 (dd, *J* = 5.3, 5.3 Hz, 2H), 7.22 (br dd, *J* = 8.8, 4.2 Hz, 1H), 7.30–7.37 (m, 2H).

2-[2-[4-Fluoro-2-(trifluoromethyl)phenoxy]ethyl]-7-(4-methyl-1*H*-imidazol-1-yl)-3,4-dihydro-2*H*-pyrido[1,2-*a*]pyrazine-1,6-dione (**50**). 5-(4-Methyl-1*H*-imidazol-1-yl)-6-oxo-1,6-dihydropyridine-2-carboxylic acid, hydrobromide salt (**34**) (201 mg, 0.729 mmol) and 2-([2-[4-fluoro-2-(trifluoromethyl)phenoxy]ethyl]amino)ethanol (214

mg, 0.801 mmol) were combined in dichloromethane (15 mL) and *N,N*-diisopropylethylamine (0.508 mL, 2.92 mmol), and the mixture was stirred for 5 min at room temperature. HATU (97%, 857 mg, 2.19 mmol) was added in one portion, and the reaction was stirred for an additional 16 h. Water (50 mL) was added, and the mixture was extracted with dichloromethane (3 × 50 mL). The combined organic layers were washed with saturated aqueous sodium bicarbonate solution (50 mL), water (50 mL), and saturated aqueous sodium chloride solution (50 mL), dried (MgSO₄), filtered, and concentrated under reduced pressure. Purification was carried out twice by chromatography on silica gel (gradient 1: 0% to 20% methanol in dichloromethane; gradient 2: 0% to 70% [10% 2 N ammonia in methanol/90% ethyl acetate] in ethyl acetate) to afford the title compound as a white solid (268 mg, 82%). LCMS *m/z* 451.0 (*M* + 1). ¹H NMR (400 MHz, CD₃OD) δ 2.24 (d, *J* = 0.9 Hz, 3H), 3.90–3.95 (m, 2H), 4.01 (dd, *J* = 5.1, 5.1 Hz, 2H), 4.32–4.37 (m, 4H), 7.21–7.26 (m, 1H), 7.25 (d, *J* = 7.8 Hz, 1H), 7.30–7.32 (m, 1H), 7.32–7.39 (m, 2H), 7.76 (d, *J* = 7.8 Hz, 1H), 8.30 (d, *J* = 1.3 Hz, 1H). ¹³C NMR (125 MHz, CDCl₃) δ 158.0, 157.3, 155.7, 155.3, 152.2, 138.3, 136.2, 134.3, 130.4, 127.5, 119.9, 119.7, 114.7, 113.8, 113.7, 108.4, 67.9, 47.9, 46.5, 40.1, 13.4. HPLC purity >95%.

1-(2-Bromoethoxy)-4-chloro-2-(trifluoromethyl)benzene. Cesium carbonate (16.60 g, 50.95 mmol) was added to a solution of 4-chloro-2-(trifluoromethyl)phenol (5.00 g, 25.4 mmol) and 1,2-dibromoethane (23.90 g, 127.2 mmol) in acetonitrile (70 mL), and the reaction was heated to 70 °C for 16 h. The mixture was allowed to cool to room temperature, diluted with ethyl acetate, and washed with water. The organic layer was dried (MgSO₄), filtered, and concentrated under reduced pressure. Purification via chromatography on silica gel (gradient: 10% to 30% ethyl acetate in heptanes) afforded the title compound as a clear viscous oil (7.05 g, 91%). GCMS *m/z* 302 (*M*⁺). ¹H NMR (400 MHz, CDCl₃) δ 7.57 (d, *J* = 2.5 Hz, 1H), 7.46 (dd, *J* = 2.5, 8.8 Hz, 1H), 6.94 (d, *J* = 8.8 Hz, 1H), 4.36 (t, *J* = 6.6 Hz, 2H), 3.66 (t, *J* = 6.6 Hz, 2H).

2-([2-[4-Chloro-2-(trifluoromethyl)phenoxy]ethyl]amino)ethanol. A solution of 1-(2-bromoethoxy)-4-chloro-2-(trifluoromethyl)benzene (7.05 g, 23.2 mmol) in 2-aminoethanol (14.20 g, 232.5 mmol) was heated to 80 °C for 4 h. The reaction mixture was allowed to cool to room temperature, diluted with dichloromethane, and washed with aqueous sodium hydroxide solution (0.5 N) and water. The organic layer was dried (MgSO₄), filtered, and concentrated under reduced pressure to provide the title compound as a white solid (6.31 g, 96%). LCMS *m/z* 284.1 (*M* + 1). ¹H NMR (400 MHz, CDCl₃) δ 7.55 (d, *J* = 2.7 Hz, 1H), 7.45 (dd, *J* = 2.6, 8.9 Hz, 1H), 6.95 (d, *J* = 8.8 Hz, 1H), 4.15 (t, *J* = 5.0 Hz, 2H), 3.69–3.63 (m, 2H), 3.07 (t, *J* = 5.0 Hz, 2H), 2.89–2.84 (m, 2H).

2-[2-[4-Chloro-2-(trifluoromethyl)phenoxy]ethyl]-7-(4-methyl-1H-imidazol-1-yl)-3,4-dihydro-2H-pyrido[1,2-*a*]pyrazine-1,6-dione (51). HATU (15.7 g, 40.5 mmol) was added to a solution of 5-(4-methyl-1H-imidazol-1-yl)-6-oxo-1,6-dihydropyridine-2-carboxylic acid, hydrobromide salt (34) (4.85 g, 16.2 mmol), 2-([2-[4-chloro-2-(trifluoromethyl)phenoxy]ethyl]amino)ethanol (5.04 g, 17.2 mmol), and *N,N*-diisopropylethylamine (8.62 mL, 2.92 mmol) in dichloromethane (100 mL). The reaction was stirred at room temperature for 16 h, whereupon it was diluted with dichloromethane and washed with a saturated aqueous solution of sodium bicarbonate and with water. The organic layer was dried (MgSO₄), filtered, and concentrated under reduced pressure. Purification was carried out twice by chromatography on silica gel (gradient: 0% to 30% methanol in dichloromethane) to afford the title compound as a white solid (4.01 g, 53%). LCMS *m/z* 467.1 (*M* + 1). ¹H NMR (400 MHz, CD₃OD) δ 2.24 (d, *J* = 0.9 Hz, 3H), 3.90–3.94 (m, 2H), 4.01 (dd, *J* = 5.1, 5.0 Hz, 2H), 4.32–4.39 (m, 4H), 7.21–7.27 (m, 2H), 7.30–7.32 (m, 1H), 7.56–7.60 (m, 2H), 7.76 (d, *J* = 7.7 Hz, 1H), 8.30 (d, *J* = 1.3 Hz, 1H). ¹³C NMR (125 MHz, CDCl₃) δ 158.1, 155.7, 154.6, 138.2, 136.1, 133.3, 130.3, 127.5, 127.4, 126.1, 123.9, 121.8, 114.7, 113.7, 108.4, 67.7, 47.9, 46.5, 40.1, 13.3. HRMS: calcd for C₂₁H₁₉ClF₃N₄O₃ (*M* + H)⁺ = 467.1098, found = 467.1091. HPLC purity >95%.

[3-(2-Bromoethoxy)phenyl][4-(pent-4-yn-1-yloxy)phenyl]methanone. Dibromoethane (0.60 mL, 7.0 mmol) and cesium

carbonate (456 mg, 1.40 mmol) were added to a solution of (3-hydroxyphenyl)[4-(pent-4-yn-1-yloxy)phenyl]methanone (196 mg, 0.70 mmol) in acetonitrile (15 mL). The reaction mixture was heated to 70 °C and was stirred overnight, whereupon it was allowed to cool to room temperature. The reaction mixture was then poured into dichloromethane (25 mL), washed with water (2 × 20 mL), dried (MgSO₄), filtered, and concentrated under reduced pressure. The resulting residue was purified by chromatography on silica gel (gradient: 10% to 30% ethyl acetate in heptane) to afford the title compound (271 mg, 54%). LCMS *m/z* 387.2 (*M* + 1). ¹H NMR (CDCl₃, 400 MHz) δ 7.79 (d, *J* = 8.4 Hz, 2H), 7.29–7.37 (m, 3H), 7.10 (d, *J* = 8 Hz, 1H), 6.94 (d, *J* = 8.4 Hz, 2H), 4.32 (t, *J* = 6.2 Hz, 2H), 4.14 (t, *J* = 6.2 Hz, 2H), 3.63 (t, *J* = 6.2 Hz, 2H), 2.40 (td, *J* = 6.9, 6.9 Hz, 2H), 2.01 (m, 2H), 1.95 (m, 1H).

{3-[2-(2-Hydroxyethylamino)ethoxy]phenyl}[4-(pent-4-yn-1-yloxy)phenyl]methanone. A solution of [3-(2-bromoethoxy)phenyl][4-(pent-4-yn-1-yloxy)phenyl]methanone (147 mg, 0.38 mmol) in ethanolamine (0.23 mL, 3.8 mmol) was heated to 80 °C for 3 h. The reaction was allowed to cool to room temperature and was diluted with dichloromethane (15 mL). The mixture was washed with 0.5 N hydrochloric acid (2 × 15 mL), water (15 mL), and brine (10 mL). The organic layer was dried (MgSO₄), filtered, and concentrated under reduced pressure to provide the title compound (87 mg, 62%) as a white solid. LCMS *m/z* 368.3 (*M* + 1). ¹H NMR (CDCl₃, 400 MHz) δ 7.79 (d, *J* = 8.8 Hz, 2H), 7.34 (m, 2H), 7.28 (m, 1H), 7.08 (d, *J* = 8.4 Hz, 1H), 6.93 (d, *J* = 7.2 Hz, 2H), 4.11 (m, 4H), 3.64 (m, 2H), 3.02 (m, 2H), 2.83 (m, 2H), 2.41 (m, 2H), 2.00 (m, 3H).

7-(4-Methyl-1H-imidazol-1-yl)-2-(2-[3-[4-(pent-4-yn-1-yloxy)benzoyl]phenoxy]ethyl)-3,4-dihydro-2H-pyrido[1,2-*a*]pyrazine-1,6-dione (53). HATU (212 mg, 0.558 mmol) was added to a solution of 5-(4-methyl-1H-imidazol-1-yl)-6-oxo-1,6-dihydropyridine-2-carboxylic acid, hydrobromide salt (34) (60 mg, 0.22 mmol), {3-[2-(2-hydroxyethylamino)ethoxy]phenyl}[4-(pent-4-yn-1-yloxy)phenyl]methanone (87 mg, 0.24 mmol), and *N,N*-diisopropylethylamine (0.16 mL, 0.87 mmol) in dichloromethane (2 mL), and the reaction was stirred for 19 h at room temperature. The mixture was diluted with dichloromethane (15 mL) and washed with a saturated aqueous solution of sodium bicarbonate (15 mL) and with water (15 mL). The organic layer was dried (MgSO₄), filtered, and concentrated under reduced pressure. The resulting residue was purified by chromatography on silica gel (gradient: 0% to 40% methanol in ethyl acetate) to provide the title compound (76 mg, 63%) as a solid. LCMS *m/z* 551.2 (*M* + 1). ¹H NMR (CDCl₃) δ 1.99–2.09 (m, 3H), 2.29 (s, 3H), 2.42–2.48 (m, 2H), 3.91–3.96 (m, 2H), 3.98–4.03 (m, 2H), 4.15–4.20 (m, 2H), 4.30–4.34 (m, 2H), 4.36–4.42 (m, 2H), 6.95–7.00 (m, 2H), 7.07–7.12 (m, 1H), 7.14 (br s, 1H), 7.26–7.47 (m, 5 H, assumed; partially obscured by solvent peak), 7.79–7.83 (m, 2H), 8.23 (br s, 1H). HPLC purity >95%.

■ ASSOCIATED CONTENT

Supporting Information

The following experimental information is provided: cell-based Aβ production assay, determination of Aβ lowering activity in vivo, and photoaffinity labeling of HeLa membranes with clickable GSMs followed by Western blot analysis. This material is available free of charge via the Internet at <http://pubs.acs.org>.

■ AUTHOR INFORMATION

Corresponding Author

*Phone: (617) 395-0705. E-mail: Martin.Pettersson@pfizer.com.

Present Addresses

[§]255 W. MLK Jr. Blvd., Unit 817, Charlotte, NC 28202.

[†]Clinical Pharmacology, Takeda Pharmaceuticals, 1 Takeda Parkway, Deerfield, IL 60015.

^{||}BioDuro Shanghai, BioDuro Co., Ltd., 233 North Fute Road, Weigaoqiao Free Trade Zone, Shanghai 200131, China.

[#]Toronto Research Chemicals, 2 Brisbane Road, Toronto, Ontario M3J 2J8, Canada.

Notes

The authors declare no competing financial interest.

■ ACKNOWLEDGMENTS

We thank Stacey Becker, Emily Miller, Michael Marconi, Emily Sylvain, and Karin Wallace for their contributions to the in vivo studies. We also thank Katherine Brighty for editing the manuscript, and the Pfizer ADME technology group for generating the in vitro pharmacokinetic data to support the SAR efforts.

■ ABBREVIATIONS USED

A β , amyloid- β peptide; AD, Alzheimer's disease; ADME, absorption, distribution, metabolism, and excretion; APP, amyloid precursor protein; AB, apical to basolateral; BA, basolateral to apical; CL_{int,app}, apparent intrinsic clearance; CNS MPO, central nervous system multiparameter optimization; CSF, cerebrospinal fluid; CYP, cytochrome P450; GSM, γ -secretase modulator; HHEP, human hepatocytes; HLM, human liver microsomes; LipE, lipophilic efficiency; MDCK, Madin-Darby canine kidney; MDRI, multidrug resistance protein (P-glycoprotein, P-gp); PK, pharmacokinetic; PD, pharmacodynamic; PS, presenilin; RLM, rat liver microsomes; SAR, structure-activity relationship; TPSA, topological polar surface area

■ REFERENCES

- (1) Thies, W.; Bleiler, L. 2013 Alzheimer's disease facts and figures. *Alzheimer's Dementia* **2013**, *9*, 208–245.
- (2) Bertram, L.; Tanzi, R. E. The genetics of Alzheimer's disease. *Prog. Mol. Biol. Transl. Sci.* **2012**, *107*, 79–100.
- (3) (a) Walsh, D. M.; Selkoe, D. J. A β oligomers - a decade of discovery. *J. Neurochem.* **2007**, *101*, 1172–1184. (b) Karran, E.; Mercken, M.; De Strooper, B. The amyloid cascade hypothesis for Alzheimer's disease: an appraisal for the development of therapeutics. *Nat. Rev. Drug Discovery* **2011**, *10*, 698–712.
- (4) De Strooper, B.; Vassar, R.; Golde, T. The secretases: enzymes with therapeutic potential in Alzheimer disease. *Nat. Rev. Neurol.* **2010**, *6*, 99–107.
- (5) (a) Bateman, R. J.; Siemers, E. R.; Mawuenyega, K. G.; Wen, G.; Browning, K. R.; Sigurdson, W. C.; Yarasheski, K. E.; Friedrich, S. W.; DeMattos, R. B.; May, P. C.; Paul, S. M.; Holtzman, D. M. A γ -secretase inhibitor decreases amyloid- β production in the central nervous system. *Ann. Neurol.* **2009**, *66*, 48–54. (b) Tong, G.; Castaneda, L.; Wang, J.-S.; Sverdllov, O.; Huang, S.-P.; Slemmon, R.; Gu, H.; Wong, O.; Li, H.; Berman, R. M.; Smith, C.; Albright, C.; Dockens, R. C. Effects of single doses of avagacestat (BMS-708163) on cerebrospinal fluid A β levels in healthy young men. *Clin. Drug Invest.* **2012**, *32*, 761–769.
- (6) (a) Imbimbo, B. P.; Panza, F.; Frisardi, V.; Solfrizzi, V.; D'Onofrio, G.; Loggrosino, G.; Seripa, D.; Pilotto, A. Therapeutic intervention for Alzheimer's disease with γ -secretase inhibitors: Still a viable option? *Expert Opin. Invest. Drugs* **2011**, *20*, 325–341. (b) Sambamurti, K.; Greig, N. H.; Utsuki, T.; Barnwell, E. L.; Sharma, E.; Mazell, C.; Bhat, N. R.; Kindy, M. S.; Lahiri, D. K.; Pappolla, M. A. Targets for AD treatment: conflicting messages from γ -secretase inhibitors. *J. Neurochem.* **2011**, *117*, 359–374. (c) Schor, N. F. What the halted phase III γ -secretase inhibitor trial may (or may not) be telling us. *Ann. Neurol.* **2011**, *69*, 237–239.
- (7) Coric, V.; van Dyck, C. H.; Salloway, S.; Andreasen, N.; Brody, M.; Richter, R. W.; Soininen, H.; Thein, S.; Shiovitz, T.; Pilcher, G.; Colby, S.; Rollin, L.; Dockens, R.; Pachai, C.; Portelius, E.; Andreasson, U.; Blennow, K.; Soares, H.; Albright, C.; Feldman, H. H.; Berman, R. M. Safety and tolerability of the γ -secretase inhibitor

avagacestat in a phase 2 study of mild to moderate Alzheimer disease. *Arch. Neurol.* **2012**, *69*, 1430–1440.

- (8) Haapasalo, A.; Kovacs, D. M. The many substrates of presenilin/ γ -secretase. *J. Alzheimer's Dis.* **2011**, *25*, 3–28.

- (9) Mitani, Y.; Yarimizu, J.; Saita, K.; Uchino, H.; Akashiba, H.; Shitaka, Y.; Ni, K.; Matsuoka, N. Differential effects between γ -secretase inhibitors and modulators on cognitive function in amyloid precursor protein-transgenic and nontransgenic mice. *J. Neurosci.* **2012**, *32*, 2037–2050.

- (10) (a) Weggen, S.; Eriksen, J. L.; Das, P.; Sagi, S. A.; Wang, R.; Pietrzik, C. U.; Findlay, K. A.; Smith, T. E.; Murphy, M. P.; Bulter, T.; Kang, D. E.; Marquez-Sterling, N.; Golde, T. E.; Koo, E. H. A subset of NSAIDs lower amyloidogenic A β 42 independently of cyclooxygenase activity. *Nature* **2001**, *414*, 212–216. (b) Eriksen, J. L.; Sagi, S. A.; Smith, T. E.; Weggen, S.; Das, P.; McLendon, D. C.; Ozols, V. V.; Jessing, K. W.; Zavitz, K. H.; Koo, E. H.; Golde, T. E. NSAIDs and enantiomers of flurbiprofen target γ -secretase and lower A β 42 in vivo. *J. Clin. Invest.* **2003**, *112*, 440–449. (c) Weggen, S.; Eriksen, J. L.; Sagi, S. A.; Pietrzik, C. U.; Golde, T. E.; Koo, E. H. A β 42-Lowering nonsteroidal anti-inflammatory drugs preserve intramembrane cleavage of the amyloid precursor protein (APP) and ErbB-4 receptor and signaling through the APP intracellular domain. *J. Biol. Chem.* **2003**, *278*, 30748–30754. (d) Weggen, S.; Eriksen, J. L.; Sagi, S. A.; Pietrzik, C. U.; Ozols, V.; Fauq, A.; Golde, T. E.; Koo, E. H. Evidence that nonsteroidal anti-inflammatory drugs decrease amyloid β 42 production by direct modulation of γ -secretase activity. *J. Biol. Chem.* **2003**, *278*, 31831–31837.

- (11) (a) Pettersson, M.; Stepan, A. F.; Kauffman, G. W.; Johnson, D. S. Novel γ -secretase modulators for the treatment of Alzheimer's disease: a review focusing on patents from 2010 to 2012. *Expert Opin. Ther. Pat.* **2013**, *23*, 1349–1366. (b) Pettersson, M.; Kauffman, G. W.; am Ende, C. W.; Patel, N. C.; Stiff, C.; Tran, T. P.; Johnson, D. S. Novel γ -secretase modulators: a review of patents from 2008 to 2010. *Expert Opin. Ther. Pat.* **2011**, *21*, 205–226. (c) Oehlrich, D.; Berthelot, D. J.-C.; Gijzen, H. J. M. γ -Secretase modulators as potential disease modifying anti-Alzheimer's drugs. *J. Med. Chem.* **2011**, *54*, 669–698.

- (12) Green, R. C.; Schneider, L. S.; Amato, D. A.; Beelen, A. P.; Wilcock, G.; Swabb, E. A.; Zavitz, K. H. Effect of tarenflurbil on cognitive decline and activities of daily living in patients with mild Alzheimer disease: A randomized controlled trial. *JAMA, J. Am. Med. Assoc.* **2009**, *302*, 2557–2564.

- (13) (a) Page, R. M.; Baumann, K.; Tomioka, M.; Pérez-Revuelta, B. I.; Fukumori, A.; Jacobsen, H.; Flohr, A.; Luebbbers, T.; Ozmen, L.; Steiner, H.; Haass, C. Generation of A β 38 and A β 42 is independently and differentially affected by familial Alzheimer disease-associated presenilin mutations and γ -secretase modulation. *J. Biol. Chem.* **2008**, *283*, 677–683. (b) Ohki, Y.; Higo, T.; Uemura, K.; Shimada, N.; Osawa, S.; Berezovska, O.; Yokoshima, S.; Fukuyama, T.; Tomita, T.; Iwatsubo, T. Phenylpiperidine-type γ -secretase modulators target the transmembrane domain 1 of presenilin 1. *EMBO J.* **2011**, *30*, 4815–4824. (c) Crump, C. J.; Fish, B. A.; Castro, S. V.; Chau, D.-M.; Gertsik, N.; Ahn, K.; Stiff, C.; Pozdnyakov, N.; Bales, K. R.; Johnson, D. S.; Li, Y.-M. Piperidine acetic acid based γ -secretase modulators directly bind to presenilin-1. *ACS Chem. Neurosci.* **2011**, *2*, 705–710.

- (14) (a) Hashimoto, T.; Ishibashi, A.; Hagiwara, H.; Murata, Y.; Takenaka, O.; Miyagawa, T. E2012: A novel gamma-secretase modulator - pharmacology. *Alzheimer's Dementia* **2010**, *6* (Suppl), S242. (b) Portelius, E.; Van Broeck, B.; Andreasson, U.; Gustavsson, M. K.; Mercken, M.; Zetterberg, H.; Borghys, H.; Blennow, K. Acute effect on the A β isoform pattern in CSF in response to γ -secretase modulator and inhibitor treatment in dogs. *J. Alzheimer's Dis.* **2010**, *21*, 1005–1012.

- (15) De Strooper, B.; Iwatsubo, T.; Wolfe, M. S. Presenilins and γ -secretase: structure, function, and role in Alzheimer disease. *Cold Spring Harbor Perspect. Med.* **2012**, *2*, a006304.

- (16) (a) Crump, C. J.; Johnson, D. S.; Li, Y.-M. Development and mechanism of γ -secretase modulators for Alzheimer's disease. *Biochemistry* **2013**, *52*, 3197–3216. (b) Pozdnyakov, N.; Murrey, H. E.; Crump, C. J.; Pettersson, M.; Ballard, T. E.; am Ende, C. W.; Ahn,

- K.; Li, Y.-M.; Bales, K. R.; Johnson, D. S. γ -Secretase modulator (GSM) photoaffinity probes reveal distinct allosteric binding sites on presenilin. *J. Biol. Chem.* **2013**, *288*, 9710–9720. (c) Crump, C. J.; am Ende, C. W.; Ballard, T. E.; Pozdnyakov, N.; Pettersson, M.; Chau, D.-M.; Bales, K. R.; Li, Y.-M.; Johnson, D. S. Development of clickable active site-directed photoaffinity probes for γ -secretase. *Bioorg. Med. Chem. Lett.* **2012**, *22*, 2997–3000. (d) Crump, C. J.; Johnson, D. S.; Li, Y.-M. Target of γ -secretase modulators, presenilin marks the spot. *EMBO J.* **2011**, *30*, 4696–4698. (e) Ebke, A.; Luebbbers, T.; Fukumori, A.; Shirotani, K.; Haass, C.; Baumann, K.; Steiner, H. Novel γ -secretase enzyme modulators directly target presenilin protein. *J. Biol. Chem.* **2011**, *286*, 37181–37186. (f) Jumpertz, T.; Rennhack, A.; Ness, J.; Baches, S.; Pietrzik, C. U.; Bulic, B.; Weggen, S. Presenilin is the molecular target of acidic γ -secretase modulators in living cells. *PLoS ONE* **2012**, *7*, e30484.
- (17) Pettersson, M.; Johnson, D. S.; Subramanyam, C.; Bales, K. R.; am Ende, C. W.; Fish, B. A.; Green, M. E.; Kauffman, G. W.; Lira, R.; Mullins, P. B.; Navaratnam, T.; Sakya, S. M.; Stiff, C. M.; Tran, T. P.; Vetelino, B. C.; Xie, L.; Zhang, L.; Pustilnik, L. R.; Wood, K. M.; O'Donnell, C. J. Design and synthesis of dihydrobenzofuran amides as orally bioavailable, centrally active γ -secretase modulators. *Bioorg. Med. Chem. Lett.* **2012**, *22*, 2906–2911.
- (18) For some alternative, recent examples, see (a) Oehlrich, D.; Rombouts, F. J.; Berthelot, D.; Bischoff, F. P.; De Cleyne, M. A.; Jaroskova, L.; Macdonald, G.; Mercken, M.; Surkyn, M.; Trabanco, A. A.; Tresadern, G.; Van Brandt, S.; Velter, A. I.; Wu, T.; Gijssen, H. J. Design and synthesis of bicyclic heterocycles as potent gamma-secretase modulators. *Bioorg. Med. Chem. Lett.* **2013**, *23*, 4794–4800. (b) Chen, J. J.; Qian, W.; Biswas, K.; Yuan, C.; Amegadzie, A.; Liu, Q.; Nixey, T.; Zhu, J.; Ncube, M.; Rzas, R. M.; Chavez, F., Jr.; Chen, N.; Demorin, F.; Rumpf, S.; Tegley, C. M.; Allen, J. R.; Hitchcock, S.; Hungate, R.; Bartberger, M. D.; Zalameda, L.; Liu, Y.; McCarter, J. D.; Zhang, J.; Zhu, L.; Babu-Khan, S.; Luo, Y.; Bradley, J.; Wen, P. H.; Reid, D. L.; Koegler, F.; Dean, C., Jr.; Hickman, D.; Correll, T. L.; Williamson, T.; Wood, S. Discovery of 2-methylpyridine-based biaryl amides as gamma-secretase modulators for the treatment of Alzheimer's disease. *Bioorg. Med. Chem. Lett.* **2013**, *23*, 6447–6454. (c) Bischoff, F.; Berthelot, D.; De Cleyne, M.; Macdonald, G.; Minne, G.; Oehlrich, D.; Pieters, S.; Surkyn, M.; Trabanco, A. A.; Tresadern, G.; Van Brandt, S.; Velter, I.; Zaja, M.; Borghys, H.; Masungi, C.; Mercken, M.; Gijssen, H. J. Design and synthesis of a novel series of bicyclic heterocycles as potent gamma-secretase modulators. *J. Med. Chem.* **2012**, *55*, 9089–9106. (d) Gijssen, H. J.; Mercken, M. γ -Secretase modulators: Can we combine potency with safety? *Int. J. Alzheimer's Dis.* **2012**, *2012*, 295207. (e) Sun, Z. Y.; Asberom, T.; Bara, T.; Bennett, C.; Burnett, D.; Chu, I.; Clader, J.; Cohen-Williams, M.; Cole, D.; Czarniecki, M.; Durkin, J.; Gallo, G.; Greenlee, W.; Josien, H.; Huang, X.; Hyde, L.; Jones, N.; Kazakevich, I.; Li, H.; Liu, X.; Lee, J.; Maccoss, M.; Mandal, M. B.; McCracken, T.; Nomeir, A.; Mazzola, R.; Palani, A.; Parker, E. M.; Pissarnitski, D. A.; Qin, J.; Song, L.; Terracina, G.; Vicarel, M.; Voigt, J.; Xu, R.; Zhang, L.; Zhang, Q.; Zhao, Z.; Zhu, X.; Zhu, Z. Cyclic hydroxyamides as amide isosteres: Discovery of oxadiazolines and oxadiazines as potent and highly efficacious γ -secretase modulators in vivo. *J. Med. Chem.* **2012**, *55*, 489–502. Also see ref 37. For comprehensive reviews, see ref 11.
- (19) Values for clogP were calculated using the BIOBYTE (www.biobyte.com) program clogP, version 4.3.
- (20) (a) Leeson, P. D.; Springthorpe, B. The influence of drug-like concepts on decision-making in medicinal chemistry. *Nat. Rev. Drug Discovery* **2007**, *6*, 881–890. (b) Ryckmans, T.; Edwards, M. P.; Horne, V. A.; Correia, A. M.; Owen, D. R.; Thompson, L. R.; Tran, I.; Tutt, M. F.; Young, T. Rapid assessment of a novel series of selective CB2 agonists using parallel synthesis protocols: A lipophilic efficiency (LipE) analysis. *Bioorg. Med. Chem. Lett.* **2009**, *19*, 4406–4409.
- (21) Wager, T. T.; Hou, X.; Verhoest, P. R.; Villalobos, A. Moving beyond rules: The development of a central nervous system multiparameter optimization (CNS MPO) approach to enable alignment of druglike properties. *ACS Chem. Neurosci.* **2010**, *1*, 435–449.
- (22) Hughes, J. D.; Blagg, J.; Price, D. A.; Bailey, S.; DeCrescenzo, G. A.; Devraj, R. V.; Ellsworth, E.; Fobian, Y. M.; Gibbs, M. E.; Gilles, R. W.; Greene, N.; Huang, E.; Krieger-Burke, T.; Loesel, J.; Wager, T.; Whiteley, L.; Zhang, Y. Physicochemical drug properties associated with in vivo toxicological outcomes. *Bioorg. Med. Chem. Lett.* **2008**, *18*, 4872–4875.
- (23) Wager, T. T.; Chandrasekaran, R. Y.; Hou, X.; Troutman, M. D.; Verhoest, P. R.; Villalobos, A.; Will, Y. Defining desirable central nervous system drug space through the alignment of molecular properties, in vitro ADME, and safety attributes. *ACS Chem. Neurosci.* **2010**, *1*, 420–434.
- (24) Chrzanowska, M.; Rozwadowska, M. D. Asymmetric synthesis of isoquinoline alkaloids. *Chem. Rev.* **2004**, *104*, 3341–3370.
- (25) Hendrickson, J. B.; Rodríguez, C. An efficient synthesis of substituted isoquinolines. *J. Org. Chem.* **1983**, *48*, 3344–3346.
- (26) Stepan, A. F.; Karki, K.; McDonald, W. S.; Dorff, P. H.; Dutra, J. K.; Dirico, K. J.; Won, A.; Subramanyam, C.; Efremov, I. V.; O'Donnell, C. J.; Nolan, C. E.; Becker, S. L.; Pustilnik, L. R.; Sneed, B.; Sun, H.; Lu, Y.; Robshaw, A. E.; Riddell, D.; O'Sullivan, T. J.; Sibley, E.; Capetta, S.; Atchison, K.; Hallgren, A. J.; Miller, E.; Wood, A.; Obach, R. S. Metabolism-directed design of oxetane-containing arylsulfonamide derivatives as γ -secretase inhibitors. *J. Med. Chem.* **2011**, *54*, 7772–7783.
- (27) Assay method adapted from published protocols: (a) Riley, R. J.; McGinnity, D. F.; Austin, R. P. A unified model for predicting human hepatic, metabolic clearance from in vitro intrinsic clearance data in hepatocytes and microsomes. *Drug Metab. Dispos.* **2005**, *33*, 1304–1311. (b) Obach, R. S. Prediction of human clearance of twenty-nine drugs from hepatic microsomal intrinsic clearance data: An examination of in vitro half-life approach and nonspecific binding to microsomes. *Drug Metab. Dispos.* **1999**, *27*, 1350–1359.
- (28) (a) Feng, B.; Mills, J. B.; Davidson, R. E.; Mireles, R. J.; Janiszewski, J. S.; Troutman, M. D.; de Morais, S. M. In vitro P-glycoprotein assays to predict the in vivo interactions of P-glycoprotein with drugs in the central nervous system. *Drug Metab. Dispos.* **2008**, *36*, 268–275. (b) A compound with a MDR efflux ratio (MDR Er) less than 2.5 is considered to have minimal P-gp efflux liability.
- (29) Callegari, E.; Malhotra, B.; Bungay, P. J.; Webster, R.; Fenner, K. S.; Kempshall, S.; LaPerle, J. L.; Michel, M. C.; Kay, G. G. A comprehensive non-clinical evaluation of the CNS penetration potential of antimuscarinic agents for the treatment of overactive bladder. *Br. J. Clin. Pharmacol.* **2011**, *72*, 235–246.
- (30) Parkinson, A.; Ogilvie, B. W. Biotransformation of Xenobiotics. In *Casarett & Doull's Toxicology, The Basic Science of Poisons*, 7th ed.; Klaassen, C. D., Ed.; The McGraw-Hill Co., Inc.: New York, 2008; Chapter 6, pp 161–304. Also available online: <http://ilmufarmasis.files.wordpress.com/2011/07/casarett-and-doulls-toxicology-the-basic-science-of-poisons7th-ed.pdf> (accessed Oct 23, 2013).
- (31) (a) Wai, J. S.; Kim, B.; Fisher, T. E.; Zhuang, L.; Embrey, M. W.; Williams, P. D.; Staas, D. D.; Culbertson, C.; Lyle, T. A.; Vacca, J. P.; Hazuda, D. J.; Felock, P. J.; Schleif, W. A.; Gabryelski, L. J.; Jin, L.; Chen, I.-W.; Ellis, J. D.; Mallai, R.; Young, S. D. Dihydroxypyridopyrazine-1,6-dione HIV-1 integrase inhibitors. *Bioorg. Med. Chem. Lett.* **2007**, *17*, 5595–5599. (b) Kawahara, N.; Nakajima, T.; Itoh, T.; Ogura, H. A Synthesis of pyrido[1,2-*a*]quinoxalines and pyrido[1,2-*a*]pyrazines. *Heterocycles* **1983**, *20*, 1721–1725.
- (32) HATU: O-(7-azabenzotriazol-1-yl)-N,N,N',N'-tetramethyluronium hexafluorophosphate.
- (33) Tran, T. P.; Mullins, P. B.; am Ende, C. W.; Pettersson, M. Synthesis of pyridopyrazine-1,6-diones from 6-hydroxypicolinic acids via a one-pot coupling/cyclization reaction. *Org. Lett.* **2013**, *15*, 642–645.
- (34) am Ende, C. W.; Johnson, D. S.; O'Donnell, C. J.; Pettersson, M. Y.; Subramanyam, C. Preparation of heteroaryl imidazoles and heteroaryl triazoles as γ -secretase modulators. WO2011048525A1, 2011.
- (35) Assay method adapted from published protocol: Hay, T.; Jones, R.; Beaumont, K.; Kemp, M. Modulation of the partition coefficient between octanol and buffer at pH 7.4 and pKa to achieve the optimum

balance of blood clearance and volume of distribution for a series of tetrahydropyran histamine type 3 receptor antagonists. *Drug Metab. Dispos.* **2009**, *37*, 1864–1870.

(36) Solubility was measured by Analiza, Inc., Cleveland, OH. (<http://analiza.com/physchem/logd.html#qf>).

(37) Borgegard, T.; Jureus, A.; Olsson, F.; Rosqvist, S.; Sabirsh, A.; Rotticci, D.; Paulsen, K.; Klintonberg, R.; Yan, H.; Waldman, M.; Stromberg, K.; Nord, J.; Johansson, J.; Regner, A.; Parpal, S.; Malinowsky, D.; Radesater, A. C.; Li, T.; Singh, R.; Eriksson, H.; Lundkvist, J. First and second generation gamma-secretase modulators (gsm) modulate amyloid-beta (abeta) peptide production through different mechanisms. *J. Biol. Chem.* **2012**, *287*, 11810–11819.

(38) Lapinsky, D. J. Tandem photoaffinity labeling-bioorthogonal conjugation in medicinal chemistry. *Bioorg. Med. Chem.* **2012**, *20*, 6237–6247.

(39) GSM 54 refers to a proprietary GSM containing the same pyridone imidazole core as GSM 52, but a structurally distinct right-hand fragment attached to the lactam nitrogen.